EASTERN APHRODITE TERRA ON VENUS: CHARACTERISTICS, STRUCTURE, AND MODE OF ORIGIN*

L. S. CRUMPLER

Department of Geological Sciences, Brown University, Providence, RI, U.S.A.

Abstract. Eastern Aphrodite Terra and Western Aphrodite form an altimetrically prominent 14,000 km long part of the equatorial highlands on Venus. Several parallel linear discontinuities striking northwest across the general east-west regional strike of the highlands are mapped in the altimetric and radar image data of Eastern Aphrodite and identified on the basis of abrupt termination of rift-like central chasma, offset and segmentation of the center of the highlands, and radar image discontinuities in the lowlands to the north. These characteristics are similar to those of linear discontinuities previously mapped in Western Aphrodite in terms of length, orientation, and influence on the central highlands and adjacent lowlands.

Altimetric profiles in directions parallel to the discontinuities are regionally symmetric, more ridge-like in Eastern Aphrodite compared to the plateau-dominated form of topography in Western Aphrodite, and are characterized by alternating paired ridge-and-trough forms near their crests and on their flanks. By mapping the center of symmetry in multiple profiles, the prominent segmentation of the highland is shown to be imparted by an offset of the regional symmetry along the mapped discontinuities. These characteristics are morphologically similar to several of the large-scale characteristics of divergent plate boundaries of Earth, including mid-ocean rise crests and rifts, offset at fracture zones and transform faults, and symmetric thermal boundary layer topography.

The altitude of the surface in profiles parallel to the discontinuities decreases as the square root of distance from the symmetry axes and with a slope similar to that predicted for thermal boundary layer topography associated with rates of divergence on Venus of $\sim 1 \pm 0.5$ cm/yr. In order to test the hypothesis that the linear discontinuities are analogous to fracture zones, the predicted altitude of the surface at great distance from the centers of symmetry of the central highland and in directions across the discontinuities was calculated on the basis of a thermal boundary layer topography model with offset of altimetric symmetry at each discontinuity. Similarity of observed Arecibo high-resolution altimetric profiles across the discontinuities with that calculated for thermal boundary layer topography offset by transform faults reveals that in terms of the sense and magnitude of regional steps in altimetry across discontinuities and the altitude of the surface, Eastern Aphrodite is similar to the known characteristics of crustal spreading at divergent boundaries. The plateau-like form of Western Aphrodite and the ridge-like form of Eastern Aphrodite are analogous respectively to the difference between areas of anomalous (Iceland) and normal crustal production along rise crests on Earth. Estimates of volumetric differences in crustal production in the environment of Venus and as it would be influenced by differences in mantle temperature beneath Western and Eastern Aphrodite imply that Eastern Aphrodite represents normal crustal production. On this basis, Western Aphrodite may be characterized by a mantle temperature that is warmer than the mantle beneath Eastern Aphrodite Terra, perhaps in association with deep convective mantle upwelling.

1. Introduction

The equatorial latitudes of Venus are characterized by several altimetrically high-standing regions referred to informally as the Equatorial Highlands (Phillips *et*

* 'Geology and Tectonics of Venus', special issue edited by Alexander T. Basilevsky (USSR Acad. of Sci., Moscow), James W. Head (Brown University, Providence), Gordon H. Pettengill (MIT, Cambridge, Massachusetts) and R. S. Saunders (J.P.L., Pasadena).

Earth, Moon, and Planets **50/51**: 343–388, 1990.

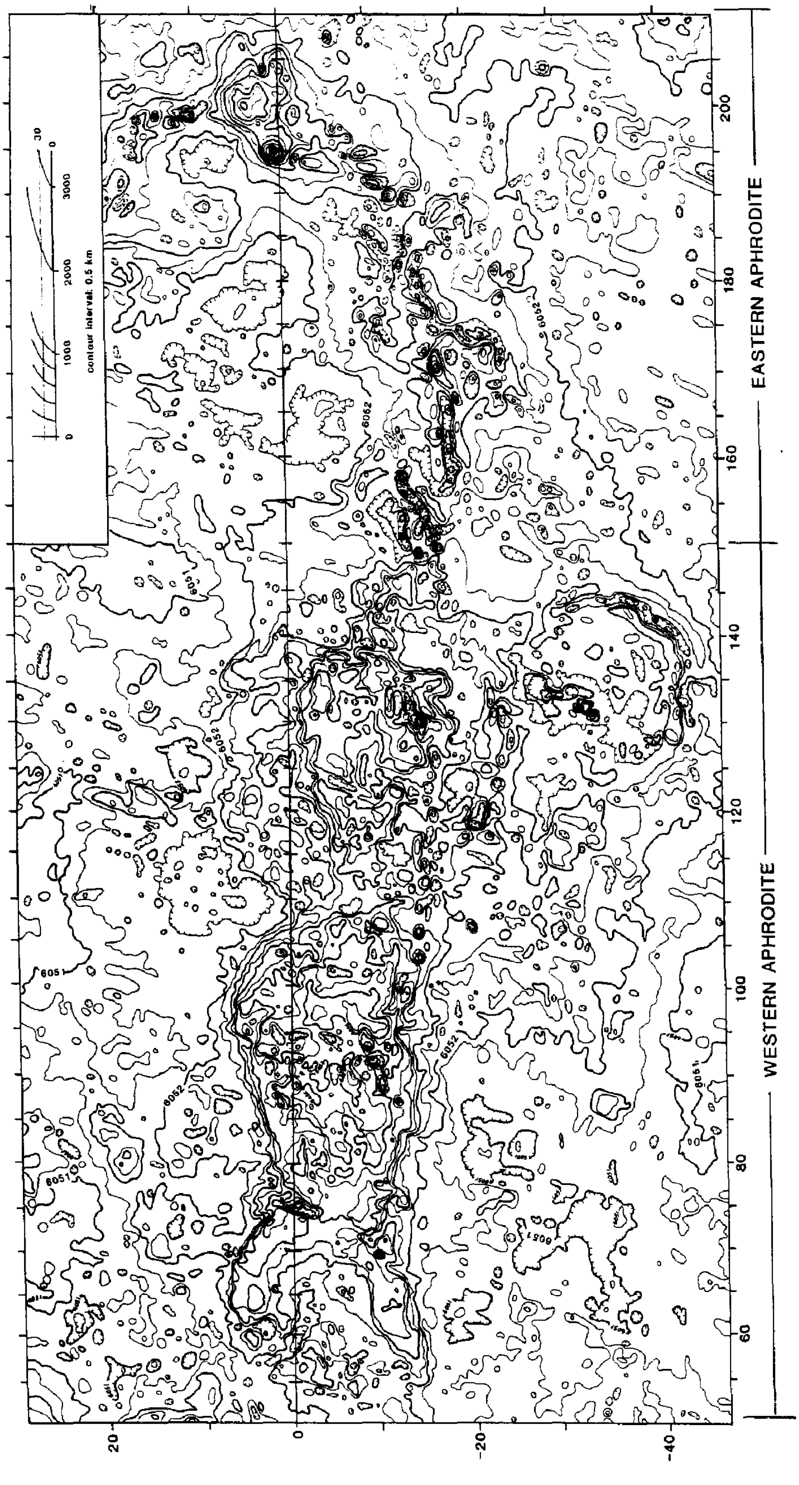
EASTERN APHRODITE
WESTERN APHRODITE
contour interval: 0.5 km
0
1000
2000
3000
20
0
-20
-40
60
80
100
120
140
160
180
200
6051
6052
6062

Fig. 1a.

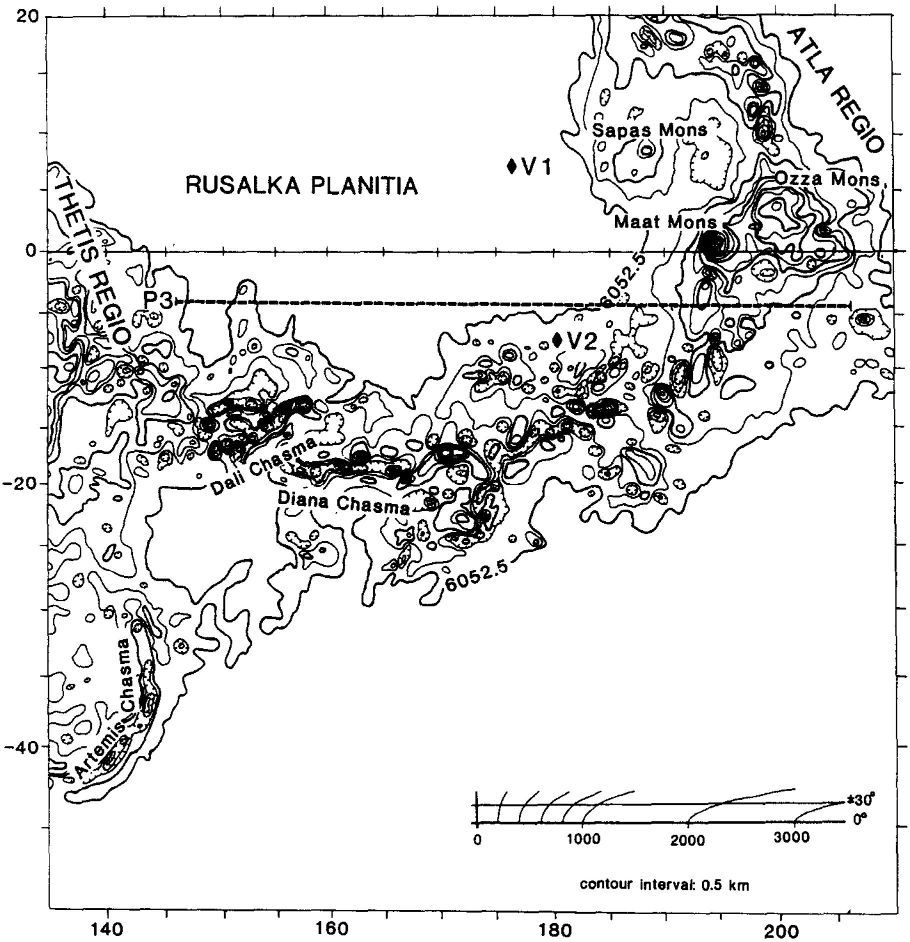

Fig. 1b.

al., 1981). The most prominent of these, as well as the largest highland on Venus, is Aphrodite Terra (Figure 1a), an elongate east-west oriented and broadly ridge-like highland surrounded by rolling lowland plains (Masursky *et al.*, 1980; Ehmann, 1983). The strong positive correlation between gravity and topography (Sjogren *et al.*, 1983; Reasenberg *et al.*, 1981) and an apparent depth of compensation typically greater (100 to several hundred kilometers) than values plausibly associated with crustal density anomalies (Bowin, 1983; Herrick *et al.*, 1989; Kiefer *et al.*, 1986; Saunders *et al.*, 1988) are cited as evidence that large segments of the Equatorial Highlands are supported by thermal or dynamic mechanism rather than Airy isostasy. Some areas of Equatorial Highlands (Western Aphrodite) are characterized by topographic rises several thousand kilometers across or by wide plateaus rising above relatively smooth rolling plains. Further west the Equatorial Highlands form broad rises accompanied by a variety of volcanics features (flows and calderas) and large volcanic constructs (Senske, 1989; Campbell *et al.*, 1989).

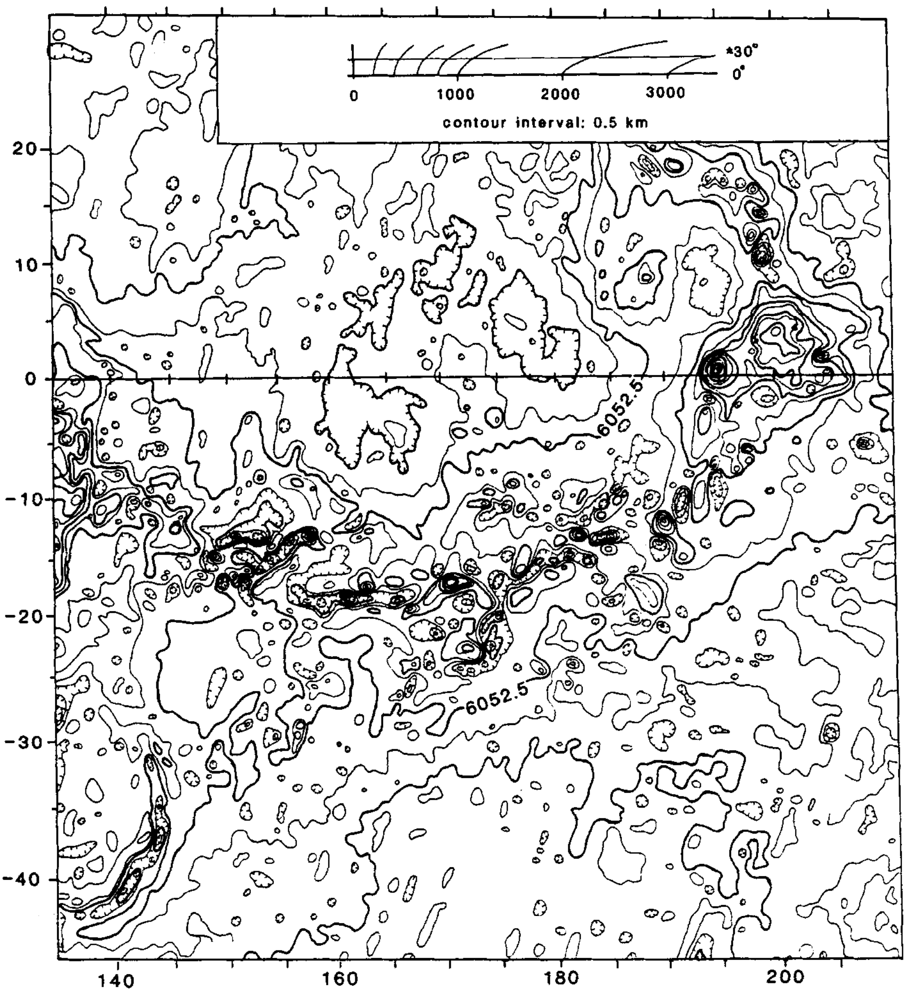

Fig. 1c.

Some of the regional aspects of the Beta Regio (Stofan *et al.*, 1989; McGill *et al.*, 1981), Eisila Regio (Senske, 1989), and the Western Aphrodite Terra parts of the Equatorial Highlands (Crumpler and Head, 1988; Crumpler and Head, 1990) have been the subject of previous geologic analyses, but the Equatorial Highlands east of longitude 150° E (referred to here as Eastern Aphrodite Terra) (Figure 1) has been studied only to a limited degree (McGill *et al.*, 1983; Schaber, 1982) and its origin and relation to the rest of the Equatorial Highlands remains incompletely known. On the basis of altimetric and surface radar properties, Eastern Aphrodite forms a saddle-shaped elongate ridge connecting the plateaus (Ovda and Thetis Regio) of Western Aphrodite and the domical broad equatorial rise of Atla Regio the crest of which is approximately 2 km above the surrounding lowland plains. Eastern Aphrodite Terra is also of note because of the common occurrence there

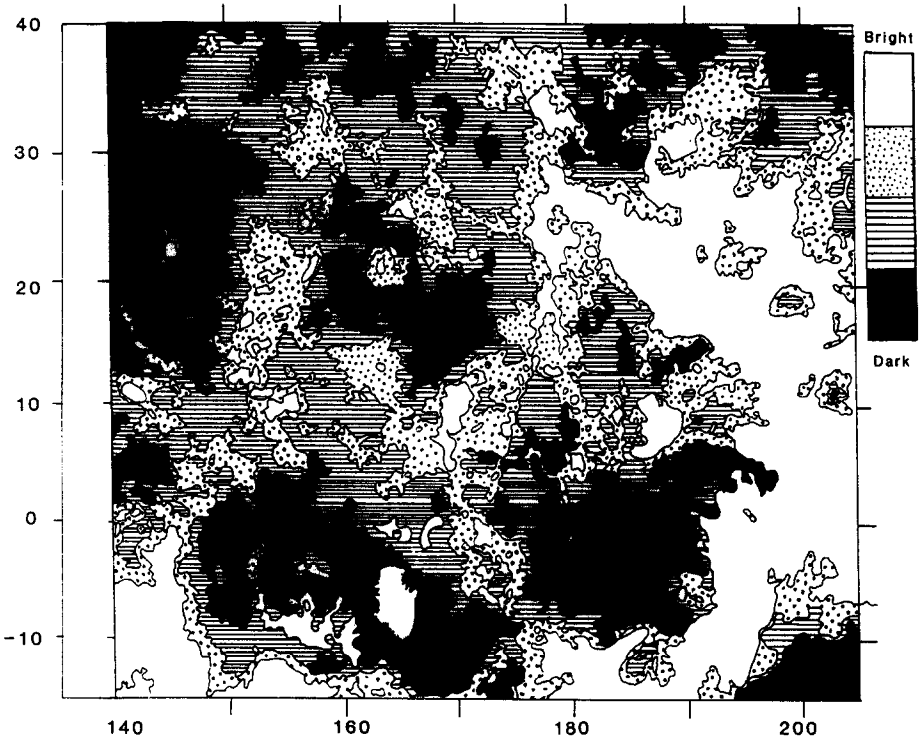

Fig. 1d.

of a prominent series of long and deep troughs or chasmata generally arrayed along or near the ridge crest and comparable in many respects with the known altimetric, morphologic, and structural characteristics of rifts in extensional tectonic settings (McGill *et al.*, 1981; Schaber, 1982). In general, an extensional tectonic environment may be a fundamental characteristic of much of the equatorial region of Venus (Head, 1986; Head and Crumpler, 1989; Schaber, 1982).

In the following we analyze some of the fundamental characteristics of Eastern Aphrodite Terra by comparing these observations and interpretations with those previously determined from other parts of the Equatorial Highlands, including Western Aphrodite Terra (Crumpler and Head, 1988; Crumpler and Head, 1990; Grimm and Solomon, 1989; Sotin *et al.*, 1989). On the basis of recent advances in current knowledge about this part of Venus, including geophysical interpretations of LOS gravity characteristics, VEGA lander surface geochemical data (Barsukov *et al.*, 1986) from Eastern Aphrodite Terra, and new high-resolution Arecibo altimetry profiles of Eastern Aphrodite Terra, and on the basis of detailed analysis and interpretations of these data, in this study we frame some fundamental questions and predictions regarding the nature of this region of the Equatorial Highlands that are testable with MAGELLAN data.

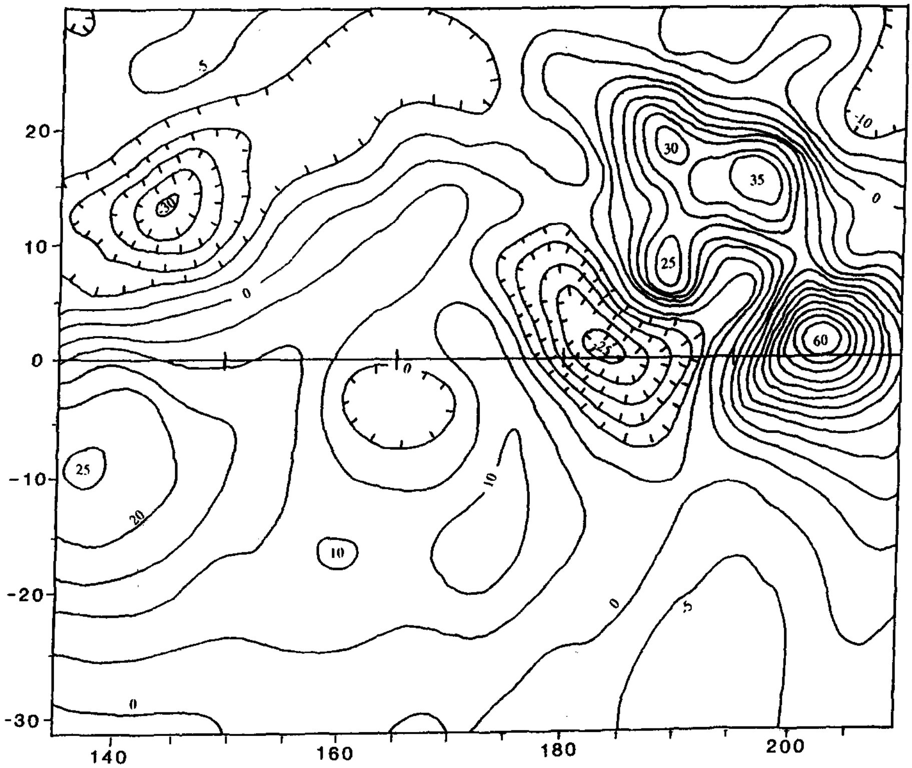

Fig. 1e.

Fig. 1. (a) Altimetric map of Western and Eastern Aphrodite. The division between east and west occurs between longitudes 140° and 150° where there is a significant change in morphology from plateaus on the west to a linear ridge on the east. (b) Altimetric map of the highland part of Eastern Aphrodite Terra and prominent named features. Areas below the 6052.5 km contour removed in order to illustrate the ridge-like regional morphology and topographic distinction in relation to the surrounding lowland plains of Eastern Aphrodite Terra. V1 and V2 refer to location of VEGA 1 and 2 landers. Line P3 shows location of high-resolution Arecibo altimetry profile track. (c) Detailed altimetric map of Eastern Aphrodite Terra including lowlands. (d) Shaded map representation of SAR image (Masursky *et al.*, 1980), Eastern Aphrodite. Altimetric contour maps constructed for this study are contoured at 0.5 kilometer altitude intervals from Pioneer Venus data gridded at 1° × 1°. (e) Line-of-sight gravity for Eastern Aphrodite (Sjogren *et al.*, 1983) showing the relatively small positive anomaly (10 mgal) associated with the saddle-shaped central part of Eastern Aphrodite. Large positive anomalies associated with eastern Thetis Regio (25 mgal), on the left, and Atla Regio (60 mgal), on the right, are among the largest anomalies in the Equatorial Highlands.

2. Altimetric, Radar Image, and Surface Chemistry Data and Results in Eastern Aphrodite Terra

Six different data sets provide constraints on the nature of Eastern Aphrodite Terra: (i) Pioneer Venus altimetric mapping, (ii) Pioneer Venus SAR imaging, (iii) Pioneer Venus RMS slope and reflectivity mapping, (iv) Pioneer Venus line-of-sight (LOS) gravity, (v) Arecibo high-resolution altimetric profiling, and (vi) VEGA lander surface chemical analyses. In the following some of the general characteristics and significant observations from each data set are examined in order to assess their individual contribution to the regional analysis

2.1. Pioneer Venus Data

The Pioneer Venus data includes near global coverage of altimetric and regional radar characteristics of the surface as well as gravity data at moderate resolutions in the low latitudes (Pettengill *et al.*, 1980; Pettengill and Ford, 1985). Based on altimetry maps derived from the Pioneer Venus data, an abrupt transition in the nature of the Equatorial Highlands and a significant division in the topographic form of Aphrodite Terra occurs around 150° E near the eastern margin of Thetis Regio and provides a natural point for distinguishing between Eastern Aphrodite Terra (150° E to 210° E) (Figure 1a) and Western Aphrodite Terra (60° E to 150° E). Eastern Aphrodite Terra is distinguished from adjacent parts of the Equatorial Highlands by its narrow ridge-like form (Figure 1b) with a gradual transition from the highland to the surrounding lowlands to the north and south, abundance of circular or domical peaks along its crest (Senske, 1989), and deep linear troughs or chasmata along the approximate ridge crest (Schaber, 1982; McGill *et al.*, 1981). Chasmata are several tens of kilometers across, 1 to 3 km deep, 1000 to 2000 km long, and form some of the steepest slopes and lowest points on Venus. Locally chasmata are flanked by adjacent parallel ridges from one to two kilometers high (Figures 1b, c) forming ridge-trough-ridge arrangements across the ridge and onto the adjacent flanks. The circularity, elevation, and relatively wide separation of the flanking domical peaks indicate that they are unlikely to be tectonic features. Their close proximity to the rift-like chasmata (Figures 1b, c) and similarity to the known characteristics of large volcanic edifices, such as Theia Mons in Beta Regio (Campbell *et al.*, 1984; Stofan *et al.*, 1989) and Sappho and Gula Mons (Campbell *et al.*, 1989) support their interpretation as large volcanic edifices (Senske, 1989). The topographic ridge crest together with the crestal chasmata occur in short segments that are frequently offset to the north or south such that in detail Eastern Aphrodite has a segmented overall appearance (Figure 1c).

Pioneer Venus reflectivity and roughness values of the surface in Atla Regio, on the eastern end of Eastern Aphrodite Terra, are among the highest on Venus and follows the general global correlation between high relative elevation and reflectivity (Head *et al.*, 1985). Lower relative backscatter areas of Eastern Aphrodite include areas exterior to the trough-like depressions of Diana and Dali Chasma where the crest of Aphrodite Terra is lowest. Diffuse scattering attains a maximum concentration within Diana and Dali Chasma and is similar to the high concentration of diffuse scatterers noted in association with Devana Chasma in Beta Regio (Bindschadler and Head, 1988a). Devana Chasma is interpreted to be a rift with numerous closely spaced radar-bright lineaments interpreted as fault scarps occurring along its length (Campbell *et al.*, 1984; Stofan *et al.*, 1989). The high-backscatter associated with the scarps is interpreted to be related to diffusely scattering blocky talus (Bindschadler and Head, 1988a).

Pioneer Venus SAR data coverage in Eastern Aphrodite includes most of Atla Regio, the eastern end of Thetis Regio and Dali Chasma, and the lowlands to the north. The central highland part of Eastern Aphrodite between longitudes 160° to 180° lie south of the southern limit of current PV SAR data. These data reveal the spatial distribution of radar surface characteristics at resolutions of 20 to 40 km and are therefore a valuable adjunct to the altimetric, roughness, and reflectivity data sets. In general SAR images (Figure 1d) show enhanced backscatter from those areas in Eastern Aphrodite lying at elevations above the 6052.5 km particularly along the central ridge and within Atla Regio. The lowlands to the north are generally darker and complexly mottled in radar backscatter.

A primary characteristic of the Pioneer Venus orbital line-of-sight (LOS) gravity data is the strong apparent correlation of positive gravity anomalies with observed large-scale surface topography throughout the Equatorial Highlands (Phillips *et al.*, 1981; Sjogren *et al.*, 1983). Atla Regio dominates the gravity signal for this part of the Equatorial Highlands (Figure 1e) where the anomaly values approach those of Beta Regio. In contrast, the saddle-shaped part of Eastern Aphrodite between longitudes 140° and 190° is characterized by moderate positive anomalies. However, because the topography is relatively low in comparison with that in Atla Regio, the observed gravity values are nonetheless significant; estimates of the apparent depths of compensation are correspondingly large in this region and in the eastern end of Thetis Regio (Herrick *et al.*, 1989). The estimated depths of compensation vary substantially from place to place throughout the Equatorial Highlands (Saunders *et al.*, 1988; Herrick *et al.*, 1989) and because some estimates of compensation exceed probable thicknesses of an elastic lithosphere, the largest anomalies are suggested to be supported by dynamic compensation mechanisms perhaps in association with vigorous mantle upwelling (Sjogren *et al.*, 1983; Kiefer and Hager, 1989; Herrick *et al.*, 1989).

2.2. Arecibo altimetric profiles

Arecibo range-doppler altimetric profiling (Campbell *et al.*, 1984) has been carried out along narrow strips near the equator and one profile (Figure 1b, line P3; and Figure 5), an along-strike continuation of profile P2 from Western Aphrodite (Crumpler *et al.*, 1987), is relevant to Eastern Aphrodite Terra. Arecibo altimetric profiles of Venus are assembled from several range-doppler radar traverses along adjacent and overlapping tracks near the sub-Earth point lying within a few hundred kilometers of the equator. Range-Doppler altimetry profiles in the longitudes of Eastern Aphrodite Terra were acquired along a track between 3.3°S and 4.7°S and sample the surface altimetry at 0.15° intervals (between ~ 10 to ~ 15 km) along track. Earth-Venus range (altimetric) resolution is about 150 m. Depending on the altimetric magnitude and detailed backscatter characteristics of the surface in the off-track directions, lateral (off-track) scatter may contribute radar returns from up to about 50 km north and south of the profile track. The observed high-resolution altimetry traverses the regional slopes from the east end of Thetis Regio, across the lowland plains of Rusalka Planitia near the VEGA 2 site, and the broad rise of Atla Regio, crossing its crest near the southern distal slopes of Maat Mons.

2.3. VEGA Lander surface analyses of Aphrodite Terra

Direct observations of the surface in Eastern Aphrodite Terra were made by the VEGA 1 and 2 landers. VEGA 1 landed on the regional slopes of a broad low plain north of the main ridge of Eastern Aphrodite and west of Atla Regio, and VEGA 2 landed on the northern slopes of Eastern Aphrodite Terra (Figure 1B). Both landers assessed the potassium, uranium and thorium content of the upper few centimeters by gamma-ray spectrometry, and VEGA 2 used x-ray flourescence (XRF) to determine major elements (Barsukov *et al.*, 1986; Surkov *et al.*, 1986; Basilevsky and Surkov, 1989) (Table I). Only gamma-ray spectrometry data are available from the VEGA 1 site, but its similarity to that determined from the VEGA 2 site implies that the compositions of the surface at the two sites are generally similar. Imaging systems were not aboard either spacecraft.

XRF data from VEGA 2 site (Table I) are characterized by major element abundances similar to that of typical terrestrial mafic or basaltic rocks, that is, relatively low potassium, moderate iron content, relatively high MgO, and moderate silica wt%. These abundances, if interpreted as a terrestrial sample would yield a normative mineralogy consisting dominantly of *ab*, *an*, and *ol*. This would suggest a relatively olivine-rich (picritic) basaltic rock, possibly silica undersaturated, and representing large degrees of melting. Hess and Head (1989) show that for a peridotitic parental source composition with H_2O and CO_2 volatile constituents, melts derived at pressures of a few tens of gigapascals (kilobars) are likely to be MORB-like basaltic melts. Comparison with analyses of rock suites on Earth shows that the VEGA 2 analysis is most similar to rocks of the olivine-gabbro-norite suite, absarokites from New Guinea, and certain flood basalts (Garvin and Bryan, 1987). These comparisons are useful for a qualitative index of elemental abundances, but are difficult to assess in terms of the petrogenetic provenance because of the potential for differences in starting mantle composition and differences in petrogenesis under varying mantle P/T conditions and volatile abundances on Venus. The VEGA 2 analysis differs from the closest terrestrial chemical analogues primarily in the high wt% sulfur abundance. High sulfur contents might result from a larger primary sulfur component in magmatic gases, or could represent deuteric alteration or atmospheric weathering of low-sulfur initial compositions. In any case, the petrologic significance of the sulfur together with the assumptions about the abundance of Na_2O are examples of the uncertainties that complicate both the comparison with typical terrestrial rocks and attempts to calculate the normative mineralogy.

TABLE I

Location and surface geochemical measurements of the surface in Eastern Aphrodite Terra by VEGA 1 and 2 landers*

Lander	Vega 1	Vega 2
Latitude	8.05	−7.5
Longitude	176.9	179.8
Region	Rusalka Planitia	North flank of EAT
Elev (above MPR)	0.4 km	1.1 km
Sfc Temp	741 K	736 K
Sfc Press.	9.5 MPa	9.1 MPa
Gamma-ray spectrometry		
− K (%)	0.45 ± 0.22	0.40 ± 0.20
− U (ppm)	0.64 ± 0.47	0.68 ± 0.38
− Th (ppm)	1.5 ± 1.2	2.0 ± 1.0
XRF		
SiO_2	–	45.6 ± 3.2
TiO_2	–	0.2 ± 0.1
Al_2O_3	–	16.0 ± 1.8
Fe_2O_3	–	7.74 ± 1.1 (8.5 ± 1.3)**
MnO	–	0.14 ± 0.12
MgO	–	11.5 ± 3.7
CaO	–	7.5 ± 0.7
K_2O	–	0.1 ± 0.08
SO_3	–	4.7 ± 1.5
Cl	–	0.3

* from Barsukov *et al.*, 1986; Surkov *et al.*, 1986; Basilevsky and Surkov, 1989.
** from Kondrat'yev et al., 1987

In order to assess the regional geologic characteristics of the surfaces sampled by the VEGA landers, Bindschadler and Head (1986) and Head *et al.* (1986) determined the location of all areas in the northern hemisphere with Pioneer Venus reflectivity and RMS slope characteristics similar to that determined for the Pioneer Venus footprint covering the VEGA lander sites and surrounding regions. It was found that Pioneer Venus radar characteristics similar to those on the surface at the VEGA 2 site (at scales between 5 cm to 10 m scales) occur over nearly a quarter of the area mapped by Venera 15/16, whereas units similar to the VEGA 1 site cover less than 3% of the area. Observed geologic characteristics of these areas in Venera 15/16 images were examined and it was determined that the VEGA 1 landing site is similar to the surfaces in Venera images mapped as individual volcanic constructs and small volcanic features, whereas the VEGA 2 site is similar to areas interpreted in radar images as broad volcanic plains (Bindschadler and Head,1986).

On the basis of the surface analyses and regional radar properties of the surface, it is concluded that the surface compositions are in general consistent with dominantly basaltic-composition lava-plains origin of the surface probably covering a significant area of the surface of Venus in Eastern Aphrodite Terra. This is consistent with the widespread occurrence of volcanic plains and the great number but relatively small areas covered by individual volcanic centers. On this basis the VEGA 1 and 2 sites are either more representative of the dominant lowland plains-forming units adjacent to the highlands than surfaces typical of the largest elevated regions, or the surface physical characteristics occurring on the lower altitude domains of Aphrodite Terra are similar to those in the lowland plains.

In summary, Eastern Aphrodite Terra is a topographically complex ridge-like area of the Equatorial Highlands. The presence of deep linear chasmata similar to rifts; abundant circular domical peaks interpreted to be volcanoes; the distinctive variations in radar reflectivity, diffuse scatterers, and rms slope; and segmented large-scale appearance of the ridge crest suggest a regional fabric or structural control on the origin and evolution of the highlands. In the following sections we examine Eastern Aphrodite in detail in order to identify further detailed tectonic characteristics of Eastern Aphrodite that may provide additional insights into the origin of this part of the Equatorial Highlands.

3. Regional Structure and Morphology of Eastern Aphrodite Terra

On the basis of the detailed surface charateristics, several regional structural fabrics have been identified throughout Eastern Aphrodite Terra, including several major regional discontinuities, shifts, or offsets in the broad topographic axis. In the following we evaluate the location, orientation, and influence of these fabrics and discontinuities on the regional structure.

3.1. Linear Altimetric and SAR Image Fabric in Eastern Aphrodite Terra

Surface structural trends and fabrics were examined by identifying and mapping all linear (elongated individual features) and straight map trends (alignments of short linear features and discontinuities) on topographic maps (Figure 2a and b), and by identifying and mapping all linear contacts between areas of distinctive SAR radar image characteristics (Figure 2c and d). On the basis of these data, a significant altimetric surface fabric consisting of two orthogonal or nearly orthogonal sets (four orientations) of linear elements is identified throughout Eastern Aphrodite (Figure 2b): (i) a trend oriented approximately N20°W and a lesser trend orthogonal to this and oriented N70°E, and (ii) a linear trend oriented parallel to the orbital track orientation (~ N30° E) and another less prominent trend at right angles to this (~ N60° W). Linear patterns oriented in northwesterly directions are abundant in the western half of Eastern Aphrodite, but recognizable linear features appear to decrease east of longitude 185° E.

The presence, location, and strike of gradients of SAR surface characteristics were mapped using a 10° × 10° non-overlapping sampling window, the corresponding number and orientation of linear features then plotted as rose diagrams (Figure 2d). These show that prominent linear trends in surface radar backscatter form two orthogonal trends; one consisting of linears oriented northwest-southeast at

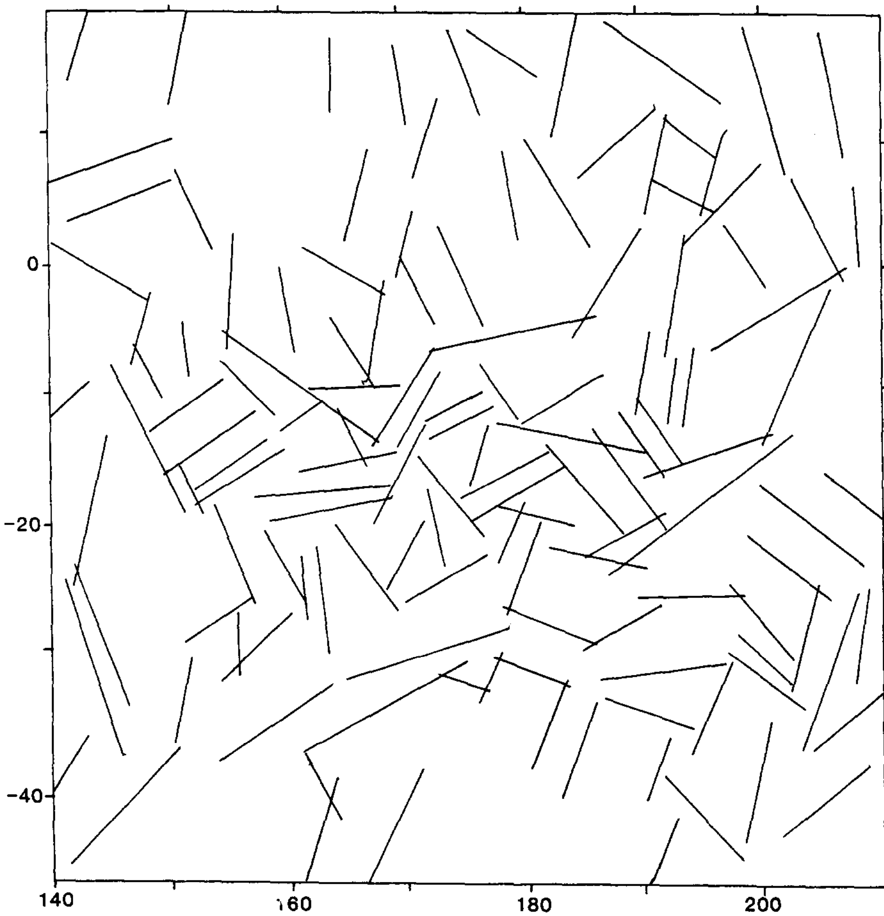

Fig. 2a.

nearly right angles to the known orientation of major linear chasmata and another trend is oriented east-northeast parallel to the chasmata. Another set is parallel and at right angles to the orbital tracks. These appear to be responsible for a northeasterly-oriented linear regional fabric in the radar image data similar to those identified previously in Western Aphrodite as artifacts of the orbital alignment of data points (Crumpler and Head, 1990).

Despite their great depth, width, and length, the chasmata are associated with the less prominent linear trend, and the northwesterly linear orientation dominates the regional fabric. This orientation also corresponds to the general trend of prominent across-strike offsets in the large scale characteristics of Eastern Aphrodite. It is concluded that the N20° W trend reflects a significant regional tectonic fabric oriented across the strike of Eastern Aphrodite Terra.

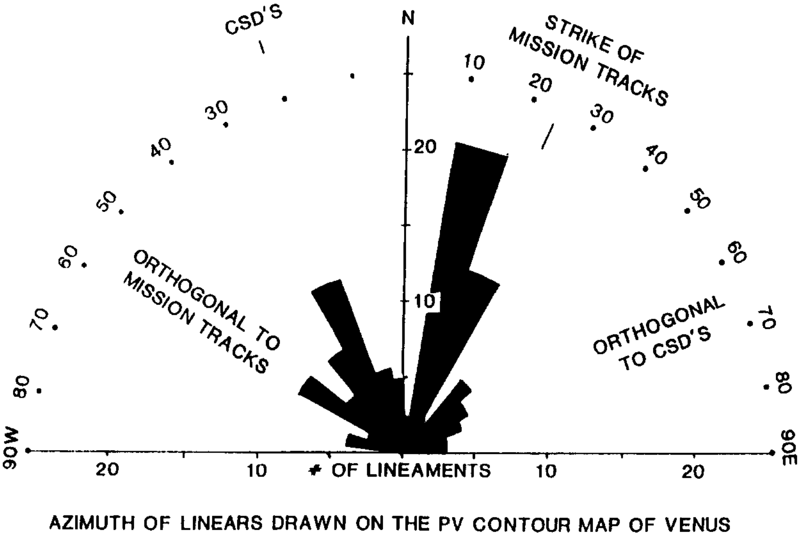
CSD'S
N
STRIKE OF MISSION TRACKS
10
20
30
40
50
60
70
80
90W
90E
ORTHOGONAL TO MISSION TRACKS
ORTHOGONAL TO CSD'S
OF LINEAMENTS
AZIMUTH OF LINEARS DRAWN ON THE PV CONTOUR MAP OF VENUS

Fig. 2b.

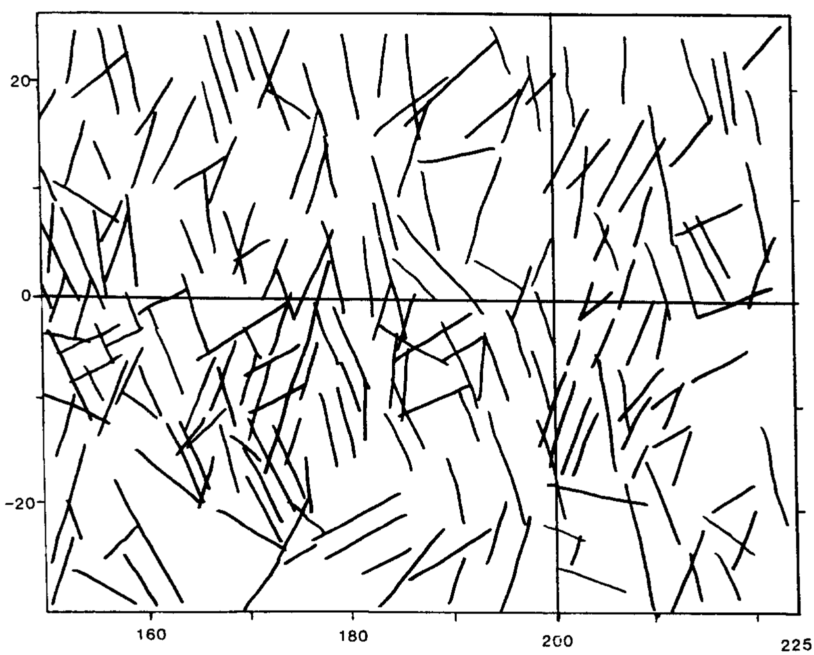
20
0
-20
160
180
200
225

Fig. 2c.

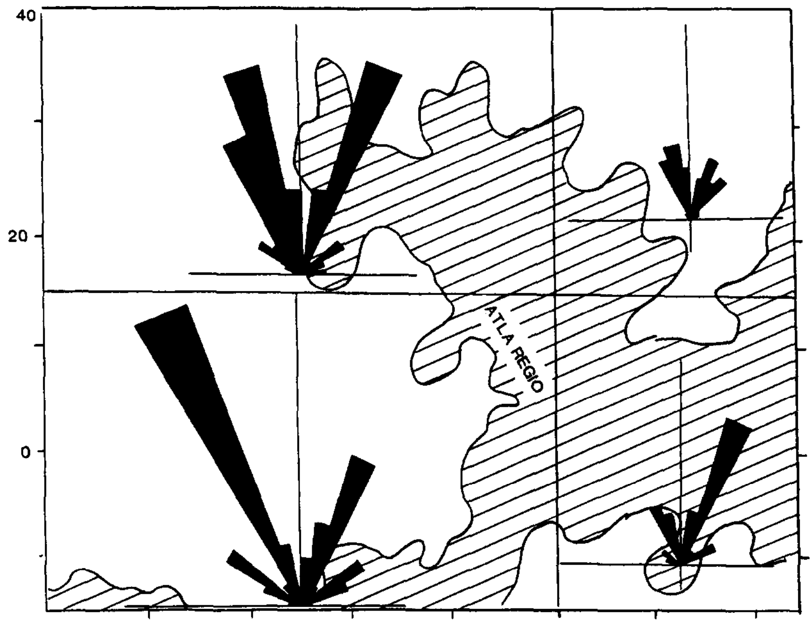

Fig. 2d.

Fig. 2. (a) Map of all linear trends identified in Eastern Aphrodite Terra from altimetric map (Figure 1a). (b) Plot of distribution of linears and their orientations as shown in (a). (c) Map of linear trends in Pioneer-Venus radar image of EAT using a 10° mapping window to confine identified linear features to those with prominent knife-edge forms. (d) Plot of distribution of orientations of SAR image linears illustrated in (c). The overall pattern of linear features in altimetric and SAR image data sets is similar to that in Western Aphrodite.

3.2. Altimetric and radar image discontinuities

The detailed across-ridge altimetry of Eastern Aphrodite Terra may be characterized as consisting in profile of a ridge with gently sloping regional flanks, a central trough or chasma with flanking ridges, and, locally, domical peaks adjacent to the central chasma (Figure 3a). Shifts in the broad topographic axis of Eastern Aphrodite Terra are associated frequently with a discontinuous segmentation of the ridges, central troughs along the crest of the ridges, and chasmata. Shifts are also noted locally by abrupt changes in SAR image characteristics. Topographically the shifts or offsets are identified by areas where margins of the ridge shifts to the north or south in the same sense and with the same horizontal magnitude as offsets in chasma segments (Figure 3b), and where there are corresponding offsets in regional slope contours on both sides of the broad topographic ridge. The high-frequency undulations in the contours is reduced and the parallel offsets and shifts in the map shape of Eastern Aphrodite is shown by portraying the 6052.5-km contour as one of sixteen permissible orientations over approximately 500 km intervals (Figure 3b, heavy black lines). The results show that the outline of

Eastern Aphrodite Terra shifts back and forth in an offset manner for several thousand kilometers.

Inspection of the high-resolution altimetry map in Figure 3b shows that few altimetric features are continuous across the trace of proposed offsets, including ridge-trough pairs. The eastern end of Diana Chasma, for example, defines a narrow zone in high-resolution altimetric maps in which the broad form of the ridge shifts southward along a trend oriented N20° W to N50° W and the western end of Dali Chasma lies approximately 500 to 600 km south along this offset zone; in detail the ends of the two chasma overlap and appear to curve toward one another. The eastern end of Dali Chasma is terminated where the broad axis of the ridge is again shifted to the south. Across this discontinuity another ridge-trough pair may be traced eastward to a similar termination, in this case where the ridge shifts to the north. Because of the discontinuous and offset nature of the ridge-trough pairs and other features, Eastern Aphrodite can be characterized as consisting of a series of segmented and offset linear chasma and parallel slope contours. These shifts or offsets all occur along narrow linear zones oriented approximately N20° W to N50° W (Figure 4a).

Several of the altimetrically mapped discontinuities described above also correlate with SAR image discontinuities (Figure 4b and Table II). The along strike projection of each discontinuity defined in Figure 4A is colinear with a prominent regional discontinuity or contact in mapped surface radar characteristics (Figure 4B) in the adjacent lowlands. For example, discontinuity **10** is parallel to the trend of a 500 km-wide and 3000 km-long radar bright feature in Rusalka Planitia, and similar smaller examples can be identified for discontinuities **9** and **14**. In reference to the cross-striking orientation and discontinuous nature of the highland with respect to these discontinuities, and in keeping with previous usage elswhere (Crumpler *et al.*, 1987), we identify these linear offset zones as cross-strike discon-

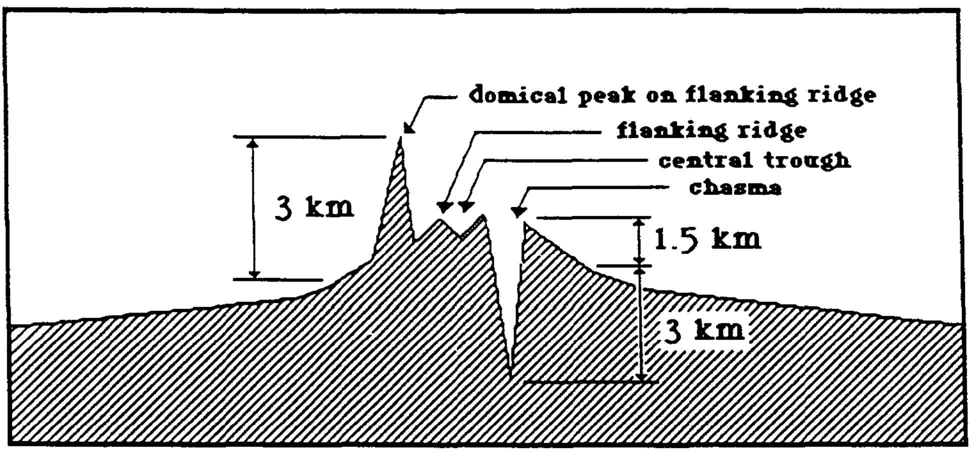

Fig. 3a.

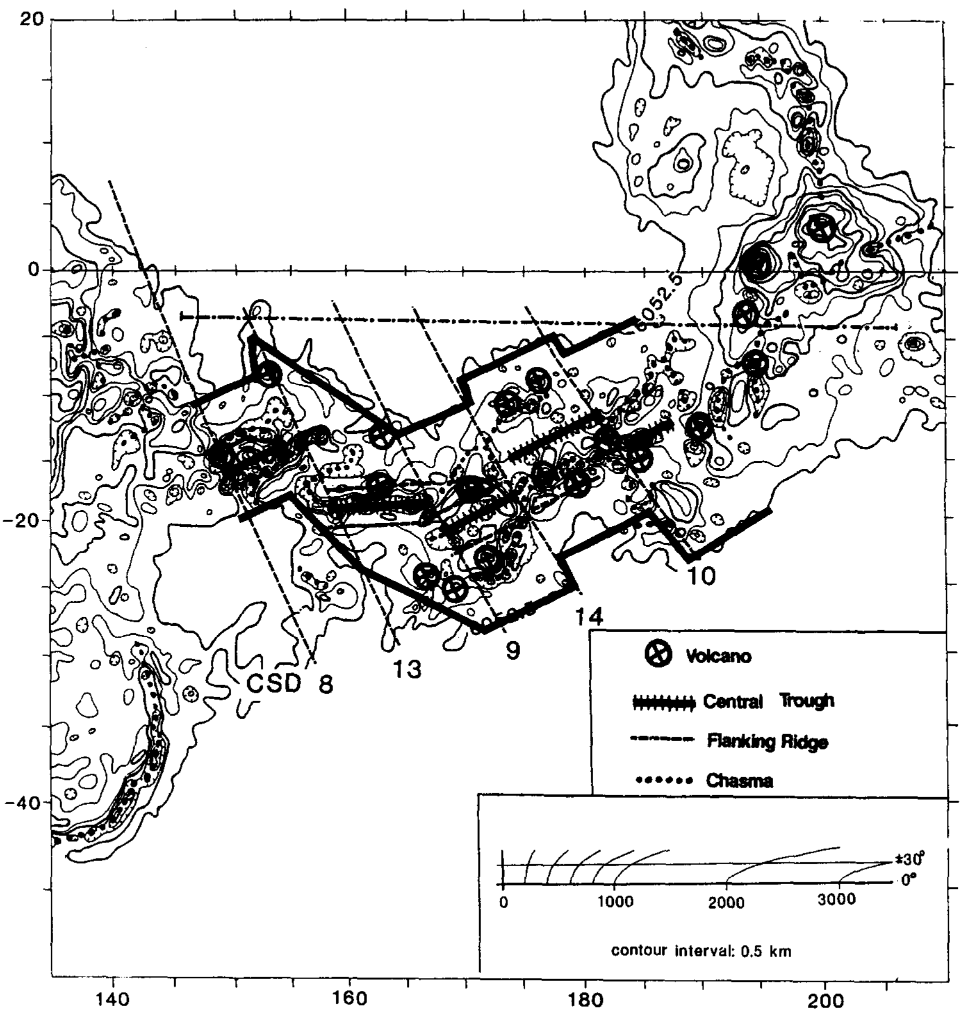

Fig. 3b.

Fig. 3. (a) Schematic drawing of general altimetric profile characteristics of Eastern Aphrodite Terra. (b) Location of distinctive altimetric features in Eastern Aphrodite includes prominent central chasmata, their adjacent ridges, and flanking domical peaks. Note that the flanks of Eastern Aphrodite appear to be parallel to the central chasmata and ridges and are offset locally in the same sense as the central chasmata. Heavy lines identify local position and general orientation of the 6052.5-km contour line as discussed in text.

tinuities (CSDs). On the basis of the correlation among offsets in morphologic, altimetric, and SAR image characteristics along the crest of Eastern Aphrodite Terra, CSDs are correlated with distinct boundaries in regional surface radar properties in both the Equatorial Highlands and the surrounding lowland plains. The overall discontinuous and offsetting configuration of CSDs results in the segmentation or generally orthogonal domain structure throughout Eastern Aphrodite (Figure 4a).

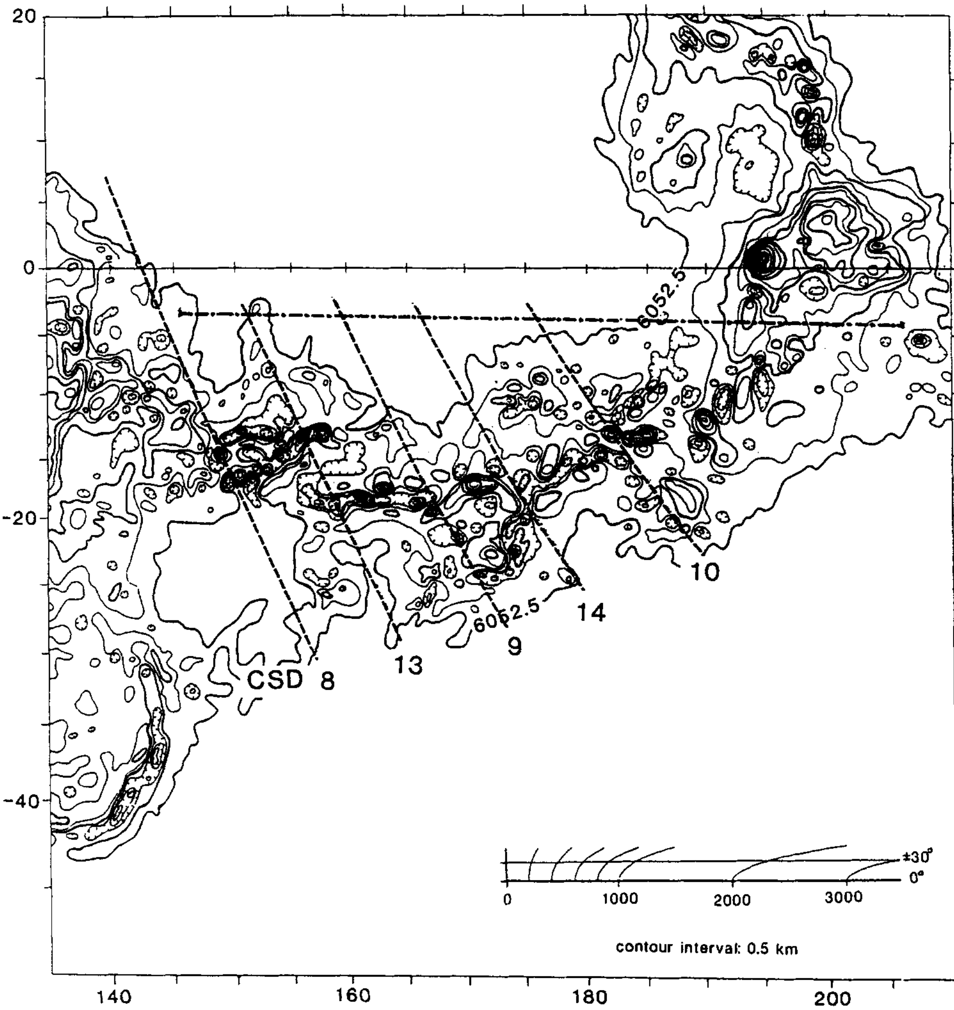

Fig. 4a.

On the basis of the combined data from altimetry and SAR image maps, CSDs in Eastern Aphrodite are on the order of 4000 km long (Table II) and, on the basis of the abruptness of changes across CSDs, the widths appear narrow with respect to regional altimetric characteristics. The across-track topographic shape and structure of individual CSDs are likely to be better resolved in high-resolution Arecibo altimetry profile. For this reason, we examine in the following the detailed structure of CSDs and domains, and their influence on regional morphologic and structural fabrics, using Arecibo altimetry profiles.

3.3. Nature of CSDs in Arecibo altimetric profiles

Significant discontinuities in surface altitude correspond to the projected along-strike intercept of CSDs with the Arecibo altimetry profile and suggest that the

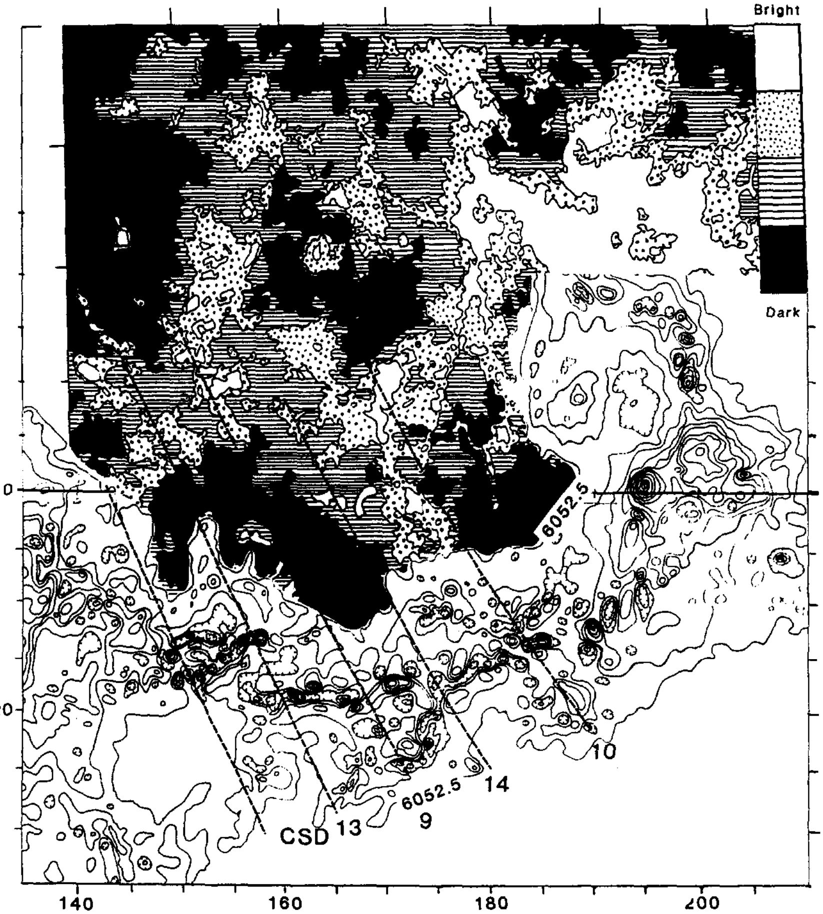

Fig. 4b.

Fig. 4. (A) Map showing location of prominent cross-strike discontinuities or CSDs (dashed lines) in relation to offsets in chasmata, paired ridges, and other discontinuous features mapped in Figure 3(B). (B) Composite map showing Pioneer-Venus radar image (SAR) brightness characteristics of Eastern Aphrodite for regions below the 6052.2 km contour and in relation to altimetric CSDs shown in (A). The northward along-strike projection of the CSDs corresponds to a variety of linear features in the SAR image of the lowlands and the CSDs are suggested to be continuous features extending from the ridge out into the lowlands. This predicts that similar characteristics may occur to the south where SAR image data is currently unavailable.

CSDs may correlate with significant high-resolution elevation discontinuities in addition to the discontinuities in cross-strike map structures (Table II). Altimetry track P3 crosses a region of the lowlands at 3 and 4 degrees south of the equator, from the slopes of the eastern margin of Thetis Regio on its western end and the southeast flank of Atla Regio on its eastern end (Figure 5). Three high-standing regional areas in the profiles [between (i) 152° E to 159° E, (ii) 166° E to 176° E, and (iii) 193° E to 204° E] correspond to areas of variable short wavelength relief,

TABLE II

Location, orientation, and characteristics of individual CSDs in Eastern Aphrodite Terra

CSD	Long. (at eq.)	Strike (NW)	Length (km)	PV/Altimetry (loc.)	PV/Altimetry (type)	PV/SAR (loc.)	PV/SAR (type)	Arecibo/Altimetry (loc.)	Arecibo/Altimetry (type)
9	158	25	4600	−13/165	L	+5/155	L	−3/159	t
				−19/165	R	+9/153	R		
				−18/165	R	+13/151	R		
				−25/172	R				
10	174	30	4300	−5/178	D	−3/176	L	−3/176	L, t
				−10/181	R	+7/171	L		
				−11/182	R				
				−14/184	R				
				−19/187	L				
13	150	23	4600	− 10/155	L, R	+4/149	L	−3/146	t
				−13/156	R	+11/145	L		
				−19/160	R				
				−21/161	R				
				−25/162	L				
				−5/152	D				
14	165	26	3800	−10/170	D	+5/161	L	−3/167	t
				−13/173	L	+3/163	R		
				−20/176	R				
				−18/177	D				
				−24/179	D, L				

Note: CSDs (1–8) described in Crumpler *et al.*, (1987) and CSDs (11–12) in Crumpler and Head (1990). Loc. = location; D = displaced contour line; L = linear slope or linear boundary; T = trough >1 km deep; t = trough <1 km deep; R = truncated trend or truncated ridge. Length based on extent shown in Figure 4B.

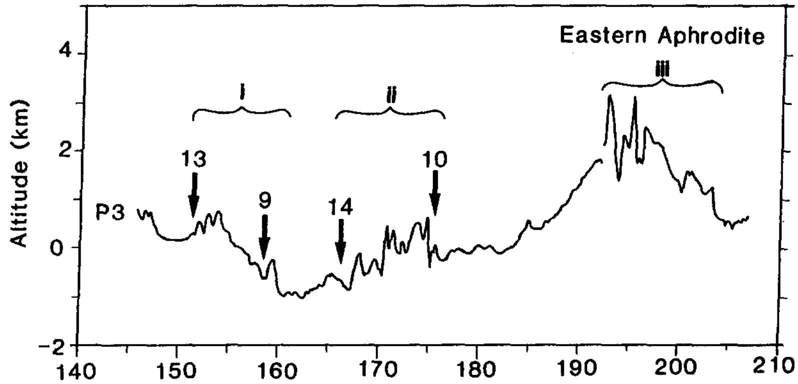

Fig. 5. High resolution Arecibo altimetry profile (P3) across the lowlands north of Eastern Aphrodite Terra. Arrows indicate projected along-strike intercept of linear discontinuities mapped in altimetric and radar image maps and shown in Figure 4. Areas denoted 'i', 'ii', and 'iii' indicate three areas with distinctive regional relief discussed in the text.

are radar bright in SAR images, and apparent in large scale altimetric maps. Areas (i) and (ii) are characterized by altimetric variations of less than a kilometer on the average and area (iii) is a part of the ridge crest along Atla Regio. Area (iii) also differs from areas (i) and (ii) in that the topographic variations are larger in amplitude and in wavelength and characterized by broader regional scale slopes.

Two potential origins of the altimetric variations and the peaks in each of these three segments of the profile are (1) variations in altitude associated with complexly faulted high-standing terrain, and (2) thermal uplifts and local volcanoes forming a broad high-standing region. The areas of locally enhanced topographic relief and roughness in the Arecibo profiles could represent samples of the detailed altimetric form of tessera in accordance with the observation that tessera are known from Venera images to be elevated tectonically complex areas (Bindschadler and Head, 1988c; Basilevsky *et al.*, 1986). Certain areas within Aphrodite Terra, notably near areas of chasmata such as Diana and Artemis, have been predicted to be most like tessera (Bindschadler *et al.*, 1990) on the basis of similarity in detailed radar backscatter characteristics. A variety of hypotheses have been considered for the origin of the tectonism associated with tessera, including topographic relaxation, compressional deformation, and seafloor spreading (Bindschadler and Head, 1988b; Head, 1990)

The VEGA 2 lander lies approximately 300 km south of the profile track and 200 to 400 km to the east of CSD **10** (Figures 4, 5) within the rolling low plains just beyond the slopes of an elevated and radar bright domain. Depending on the width of the CSD zone, and whether CSDs have distinctive surface characteristics, the VEGA 2 site could be influenced by proximity to CSD **10** and the elevated nearby plateau. The general similarity of surface XRF analyses of the surface with that at other sites, however, suggests that if differences exist they are not expressed geochemically, unless such differences are expressed by the higher local sulfur content of the surface. The topographic signature of individual CSDs where they project onto the Arecibo profile suggests that the width of the region over which the observed larger scale discontinuity takes place (width of trough or slope) is generally no wider than ~200 km. Within Atla Regio (area iii), the profiles differ from the two other rough and elevated segments in two characteristics: (1) the peaks are wider and higher and are confined to a narrow ridge crest in Atla, and (2) the local rise is dome-like as compared with the steep-sloped and plateau-like rough areas of regions (i) and (ii). At Atla Regio, several chasma, including Hecate Chasma, Ulfrun Chasma, and Ganis Chasma, merge together in a tectonic 'junction' (Senske, 1989), are similar to the locus of extensional tectonic features (rifts, volcanoes, and regional rise) which occur at Beta Regio (Stofan *et al.*, 1989; McGill *et al.*, 1981), and are similar to those associated with triple junctions on Earth. Additional prominent chasmata occur farther east in the region lying between Atla Regio and Beta Regio (Senske, 1989).

3.4. Summary of structural characteristics and origin of CSDs

CSDs are a part of a regional orthogonal tectonic fabric identifiable on the basis of several data sets (Pioneer Venus altimetry, SAR images, and Arecibo high-resolution altimetry profiles). They exert a large-scale influence on the nature of Eastern Aphrodite Terra, truncate local and regional trends in altimetry and radar properties of the surface, and define rectangular domains across which Eastern Aphrodite is segmented. Individual CSDs may be traced across the highland and well into the surrounding lowlands, are up to 4000 km long, form narrow troughs 100 to 200 km wide (Table II), and correspond to significant offsets (several hundreds of kilometers) in the broad topographic crest, associated slopes, and deep linear rift-like chasmata. CSDs therefore appear to be part of a large-scale tectonic fabric that influences the global scale characteristics of the highlands and surrounding lowlands.

On the basis of these characteristics, several origins of CSDs that may be proposed include: (i) a global tectonic grid or jointing pattern similar to that known to occur on other terrestrial planets, (ii) large strike-slip faults including faulting patterns inherited from global spin-changes (Arvidson *et al.*, 1989) as well as those resulting from horizontal tectonic movements, (iii) transform faults and fracture zones associated with 'accomodation' zones offsetting extensional fault graben and rifts (Bosworth, 1989), or (iv) fracture zones associated with offsets of thermal boundary layer topography in a plate tectonic setting.

Several characteristics of CSDs imply vertical and horizontal offsets of the surface. On the basis of the fact that regional altimetric offsets and map scale discontinuities are not a predicted characteristic of simple jointing planes at large scales, CSDs are unlikely to be the result of a planetary scale grid. The discontinuity or change in morphology of individual domains across each CSD also argue against a simple strike slip faulting origin for the north and south offset and segmentation: If the CSDs are treated as strike slip faults, attempts to restore the topography across CSDs to continuous patterns fail.

Regional topographic patterns accomodating lateral offsets in the axis of continental rifts on Earth are similar to many of the characteristics of CSDs. Rifts occur in segments and frequently, where the axis of rifting is discontinuous, the adjacent segment is offset laterally. The structural transition between the tips of the offset segments forms an 'accommodation zone' (Bosworth, 1989) across which the opposing sense of extension is accommodated and in which the detailed structural patterns indicate relative transform motion of adjacent segments.

Oceanic fracture zones are also similar to CSDs in many characteristics. Although continental rift accommodation zones originate from a transform offset similar to that associated with transform faults and fracture zones on the seafloor, there are also many fundamental differences in the regional and detailed structure associated with the origin of the two types of transform motion that may be identified in large scale maps. Because of the horizontal motion of the surface away from mid-ocean rifts, the transform motion between rifting segments of the seafloor, unlike continental rift transform offsets, is recorded in the form of long fracture zones extending up to several thousand kilometers into the abyssal plains on either side of the mid-ocean rifts. The width of accommodation zones is several kilometers and relatively diffuse or ill-defined in a structural sense, but generally no longer than the width of the rift offset. And the influence of transform zones on the local crustal production and the detailed topography resulting from offsets in the thermal boundary layer topography of divergent boundaries associated with fracture zones differs altogether from the characteristics in continental rifts where crustal production and lateral motion are minor. The symmetry of crustal accretion generally imparts a strong pattern of bilateral symmetry to the two diverging crustal halves in directions generally parallel to the fracture zone traces such that an orthogonal pattern (Macdonald, 1982; Pockalny *et al.*, 1986; Lewis, 1979) is associated with the detailed processes of crustal spreading and transform faulting. In contrast, rifts are frequently asymmetric.

In summary, CSDs appear similar in many characteristics to accommodation zones between continental type rift segments and to fracture zones and transform faults associated with crustal spreading. The presence of deep linear rift-like chasmata throughout Eastern Aphrodite Terra, the serial offset of chasmata, and the isolated peaks analogous to large volcanoes all astride a large-scale linear ridge are all characteristics of known continental rifts with associated off-axis and central-axis volcanoes and volcanic flows on Earth. But the great length of CSDs, their association with a global linear topographic rise, and the presence of approximately orthogonal regional surface fabrics are more analogous to that of fracture zones associated with crustal spreading and offset thermal boundary layer topography characteristic of the seafloor. This hypothesis may be tested by comparing the observed regional and local altimetric and radar characteristics with the predicted symmetry, length, and consistent topographic relationships predicted for crustal spreading.

4. Regional Symmetry and Topographic Relations

If CSDs are analogous to fracture zones and transform faults, a variety of symmetry features are predicted and enables a test of this hypothesis. Symmetry is predicted in this model on the basis of the fundamental symmetry of the crustal spreading process at mid-ocean ridges (Malinverno, 1990) related to the corresponding symmetry in thermal and mechanical evolution of the newly-formed lithosphere on either side of a divergent boundary in directions parallel to fracture zones and transform faults. Symmetry characteristics that are predicted include: (1) a distinctive regional bilateral symmetry parallel to the CSDs, (2) symmetry within individual domains between two CSDs, (3) offset of symmetry between domains, and (4) differences in topographic elements and in the symmetry between domains. If the CSDs are due to accommodation zones between segments of limited (continental-type) rifting, then symmetry is not required, the topography may be correlated between domains across discontinuities in a more organized manner, and CSDs should extend no farther than the offset distance between domain segments. If the CSDs represent fracture zones and transform fault associated with large-scale crustal creation and spreading, then regional symmetry is required and short wavelength symmetry may be present, the detailed topography within individual domains may differ, and the CSDs may extend for several thousand kilometers beyond the transform fault as a record of the offset in the lithosphere. In the following we evaluate the altimetry in further detail in order to assess which of these predictions better characterizes the origin and evolution of this part of the Equatorial Highlands.

In order to examine the detailed nature of altimetry in the absence of the discontinuous influences of CSDs, regional profiles across Eastern Aphrodite were constructed from traverses parallel to individual CSDs (Figure 6a). In general, these profiles are found to be broadly symmetric in directions parallel to the CSDs with a numerical correlation coefficient between the north and south flanks of profiles throughout Eastern Aphrodite of 0.75 (Table III). This symmetry may be shown and tested visually by plotting sample profiles such that each profile is paired with its mirror image in the same plot (Figure 6b). This exercise enables visualization of some of the regional symmetry that is generally present in profiles and also suggests that additional smaller elements of symmetry at shorter wavelength may be present in some. Some small scale features are notably asymmetric; for example, 'central' chasmata are frequently located within a few hundred kilometers to one side of the regional symmetry point, although a shallower depression may occur in about the same relative position with respect to the symmetry axis on the opposite flank. The values of regional (north-south profile) cross correlation for profiles in Eastern Aphrodite based on these results are comparable to those across mid-ocean ridges on the Earth (Grimm and Solomon, 1989). These values are further remarkable considering the relatively large asymmetries that are known to occur in the large-scale bathymetry of the seafloor (Hayes, 1988) and the altimetric error in the Pioneer Venus data relative to terrestrial bathymetric data.

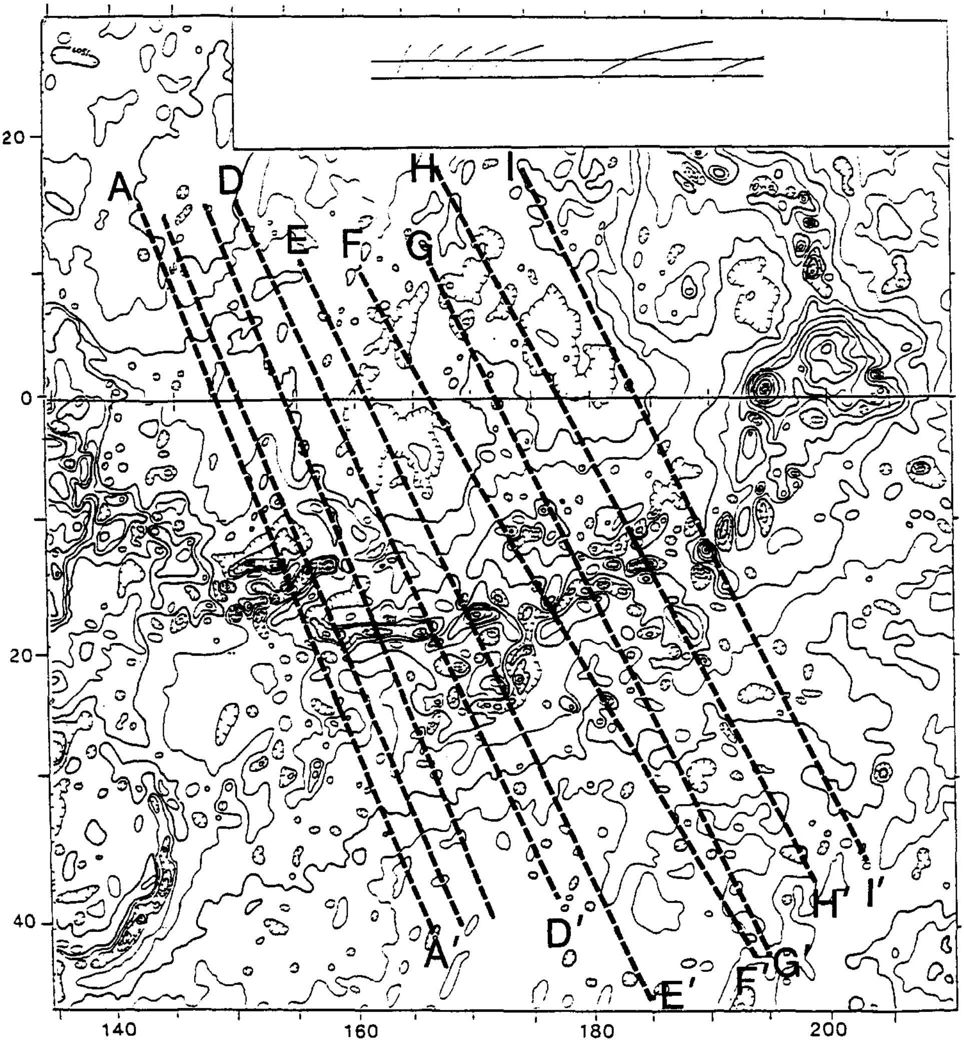

Fig. 6a.

Where small scale relief features are symmetric in profiles across ridges on the seafloor, and visually present in map representation, the symmetry may show greater cross-correlation than the regional symmetry (Grimm and Solomon, 1989). Nonetheless small scale symmetry features occur with low areal frequency on Venus and on the terrestrial seafloor. The overall contribution of this type of small-scale symmetry to the observed quantitative cross correlation on both Earth or Venus may therefore be low (Grimm and Solomon, 1989) even though small scale symmetry may be visibly present in maps (Crumpler and Head, 1990). Quantitative analysis has been found to be inadequate for evaluation of seafloor magnetic symmetry axes for similar reasons (phase differences, ridge jump history, etc.).

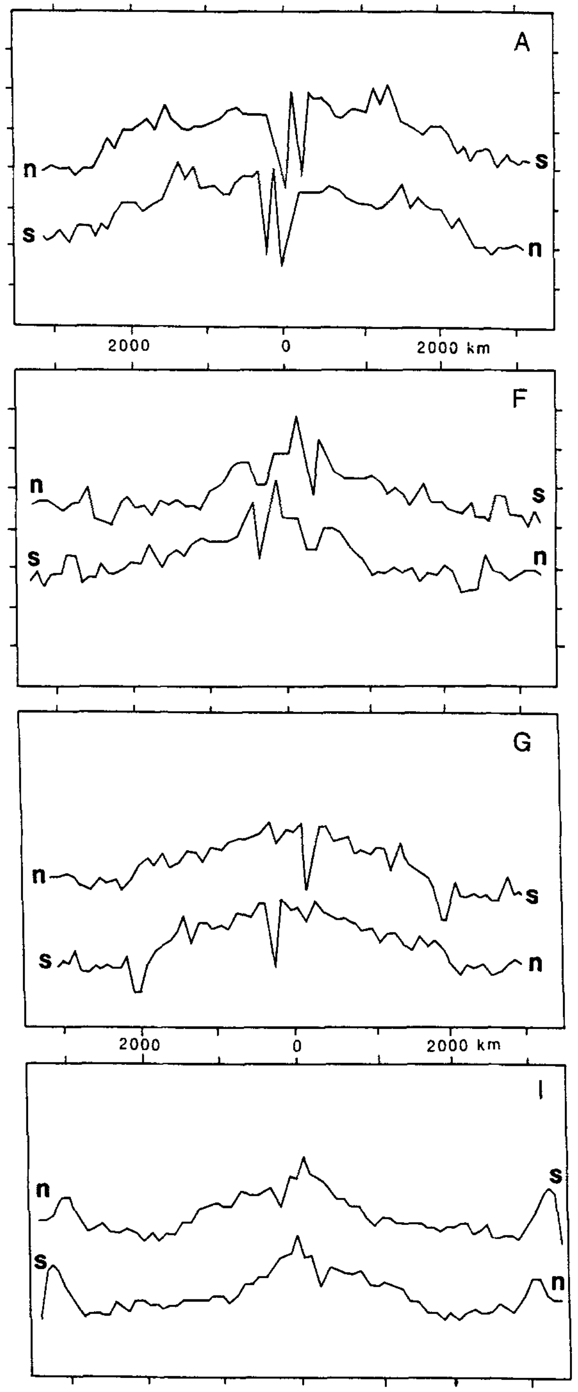

Fig. 6b.

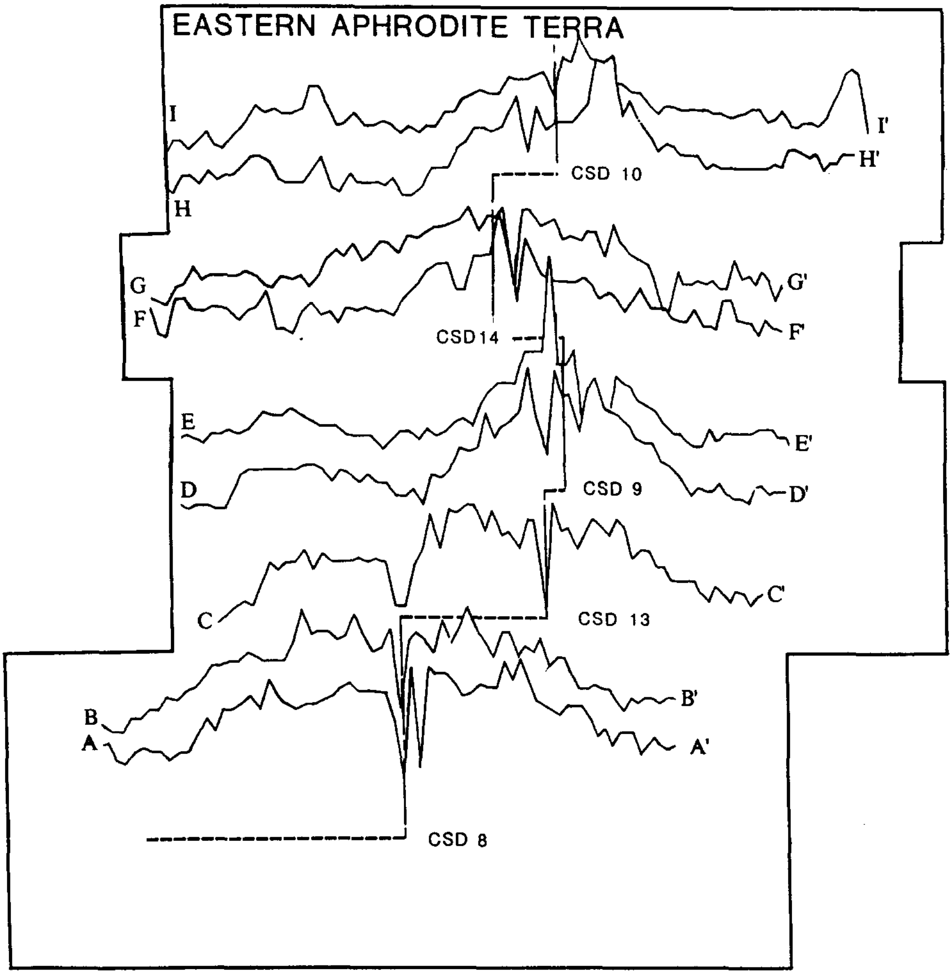

Fig. 6c.

On the basis of this type of analysis the center of large scale symmetry in each profile across Eastern Aphrodite was identified and the results enabled the identification of the relationship to adjacent linear large-scale symmetry axes when plotted beside other parallel profiles (Figure 6c). In general the axes of symmetry are linear, coincide with regional occurrences of chasmata on the ridge crest of Eastern Aphrodite, but are offset at each of the proposed CSDs (Figures 6c, d). Only a general symmetry axis is shown for the domain between CSDs **13** and **9** where the symmetry axis for profiles parallel to the CSDs shifts from north to south from west to east across the domain. In detailed resolution this apparent oblique trend can be resolved into three symmetry steps, but identifiable CSDs associated with these steps cannot be distinguished. A similar small-scale influence on perceived large-scale symmetry axis orientation was noted in gravity data from Western Aphrodite Terra (Sotin *et al.*, 1989) where multiple symmetry steps

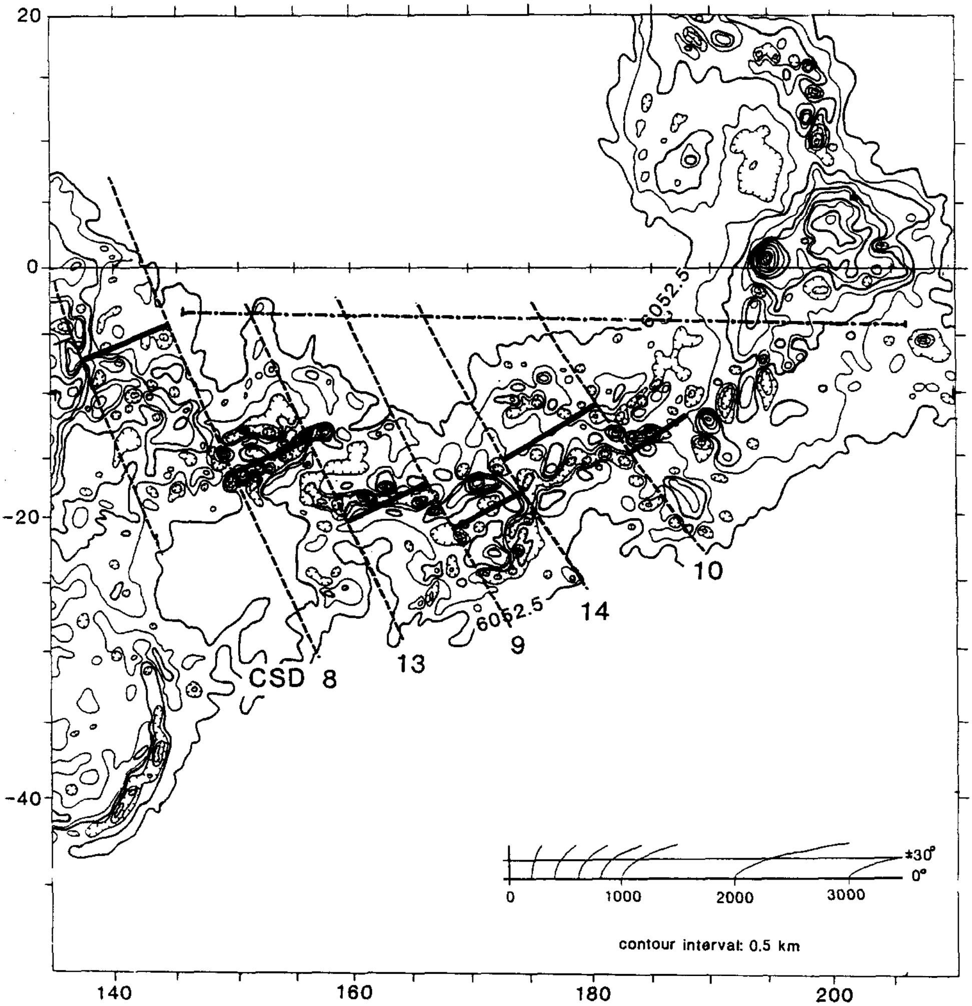

Fig. 6d.

Fig. 6. (a) Location of altimetric profile tracks (dashed lines) shown in (b, c). Profiles are taken along tracks appproximately parallel to linear discontinuities. (b) Example of four profiles illustrating the large scale symmetry across Eastern Aphrodite in directions parallel to CSDs. A mirror image of each profile is reproduced beneath each example and illustrates the quantitatively correlated large and possible small scale similarities. The average correlation coefficient for all profiles in Eastern Aphrodite Terra is 0.75. (c) Profiles arranged in their relative map positions and with respect to the regional symmetry. (d) Map of Eastern Aphrodite showing both the location of linear discontinuities and the centers of symmetry.

similar to those described here were inferred. These regional symmetry characteristics together with the presence of multiple parallel linear discontinuities define narrow corridors in altimetry characteristics and radar surface properties throughout Eastern Aphrodite that are responsible for the domain-like structure throughout Aphrodite Terra.

TABLE III

Location, rise crest height, slopes, spreading rates, and symmetry point of profiles across Aphrodite Terra

Profile	h_o	Δ	r	v	$r_{n/s}$	Endpoints [N]	[S]	Center
A_n	6054.7	0.046	0.85	2.1				
					0.62	15/142	− 45/167	− 14.5/153.6
A_s	6054.4	0.032	0.65	4.3				
B_n	6053.4	0.035	0.84	3.6				
					0.86	40/130	− 50/171	− 14/155.5
B_s	6053.4	0.036	0.82	3.4				
C_n	6054.3	0.029	0.64	5.3				
					0.71	15/148	− 45/172	− 19/161.5
C_s	6054.5	0.044	0.91	2.3				
D_n	6054.8	0.047	0.79	2.0				
					0.84	15/150	− 45/183	− 21/167
D_s	6055.3	0.069	0.92	0.9				
E_n	6053.8	0.046	0.72	2.1				
					0.96	40/138	− 50/191.5	− 19.5/170.5
E_s	6053.3	0.040	0.71	2.8				
F_n	6054.3	0.033	0.83	4.1				
					0.88	15/157	45/197	− 14/174.5
F_s	6054.5	0.039	0.88	2.9				
G_n	6053.7	0.040	0.93	2.8				
					0.47	40/149	− 50/202	− 12.5/177.5
G_s	6053.2	0.029	0.59	5.3				
H_n	6053.3	0.035	0.76	3.6				
					0.76	30/161	− 45/205	− 14/185
H_s	6053.2	0.027	0.77	6.1				
I_n	6053.1	0.023	0.67	8.3				
					0.67	30/160	45/209	− 11.5/190
I_s	6053.1	0.022	0.57	9.1				

Notes: Heights (h_0) in kilometers; Δ = observed slope, $h/\sqrt{X}$ in Eq. (3); r = correlation coefficient between h and $\sqrt{X}$; v = half-spreading rate in cm yr^{-1}; $r_{n/s}$ is the correlation coefficient between altitude values of the north and south profiles; and the end and center points of profiles are in degrees latitude/longitude. n and s subscripts designate north and south profile segments. v is calculated assuming a mantle temperature of 1500 °C. Note that the calculated half spreading rate, v, is inversely proportional to r ($r = 0.94 - 0.43 \log v$), implying that as the roughness of the profile increases, the perceived slope decreases. Values of $v \approx 0.5$ to 1.5 cm/yr are estimated to be appropriate for $r > 0.9$.

In addition to defining offset broadly symmetric domains, second order topographic elements differ in distribution and morphologic type between domains. For example, the planimetric form of symmetry within the domain lying betwen CSDs **9** and **14** (Figure 6d) consists of a broadly circular segmented shape, whereas the symmetry within adjacent domains is characterized by more linear ridge-and-trough type structures. This suggests that in addition to the regional symmetry, second order topographic elements might be symmetrically distributed.

In summary, the altimetric characteristics of Eastern Aphrodite Terra appear symmetric at a variety of scales in directions parallel to CSDs and are offset at CSDs. This implies that CSDs extend as linear parallel features for several thousand kilometers, unlike accommodation or transfer zones associated with continental style rifts, and are associated with the large-scale structure and altimetry of the Equatorial Highlands. On the basis of a variety of altimetric and structural characteristics, the extreme length of CSDs, their association with symmetry at a variety of scales, offset of this symmetry along CSDs, and differences in topographic elements of symmetry between domains across CSDs, the CSDs are considered to be analogous to fracture zones. In order to further test this hypothesis, several additional more detailed predictions and relevant tests of the hypothesis are examined in the following.

5. Analysis and Interpretation

On the basis of observed regional symmetry characteristics, a crustal spreading model for Eastern Aphrodite Terra seems plausible. If such a process is responsible for the observed features, then further tests may be made based on the following predictions that this hypothesis entails: The topography should (1) follow a general dependence on the square root of distance from a divergent boundary, (2) have a slope consistent with the predicted form of thermal boundary layer (**TBL**) topography under the surface conditions of Venus, (3) exhibit distinct discontinuities in altimetry and regional altimetric steps across these discontinuities consistent with the sense of offset of the ridge crest at fracture zones and transform faults, and (4) show evidence of crustal thickness variations expressed as linear short wavelength variations in altimetry striking parallel with the long orientation of ridge crest axes and symmetrically disposed with respect to the ridge crest. In the following we test the hypothesis further by assessing these predictions.

5.1. Fit of Topography to Linear Square-Root of Distance Relation

A predicted and observed characteristic of crustal spreading is that the surface subsides as it ages generally in accordance with the increase in thickness of a thermal boundary layer. These ideas can be tested further by examining altimetry data plotted as a function of the square root of distance north and south of the axis of symmetry from Eastern Aphrodite and in directions approximately perpendicular to the general east-west strike of the highland and parallel to CSDs (Figure 7). In these plots, the altimetry generally follows a nearly linear relationship between altitude and $\sqrt{x}$ throughout the profile. Table 3 lists the corresponding values of slope and correlations between h and $\sqrt{x}$ resulting from least squares fitting of a linear trend to the data. Because the rate of altimetric change in the upper surface of a conductively-cooled TBL is a function of the temperature difference between the surface and the base of the boundary layer, differences in the theoretical shape of TBL topography on Venus and Earth (Kaula and Phillips, 1981; Phillips and Malin, 1983) are expected. An additional smaller predicted difference is a result of the water overburden on Earth which deepens the distal seafloor relative to the ocean-free case of Venus.

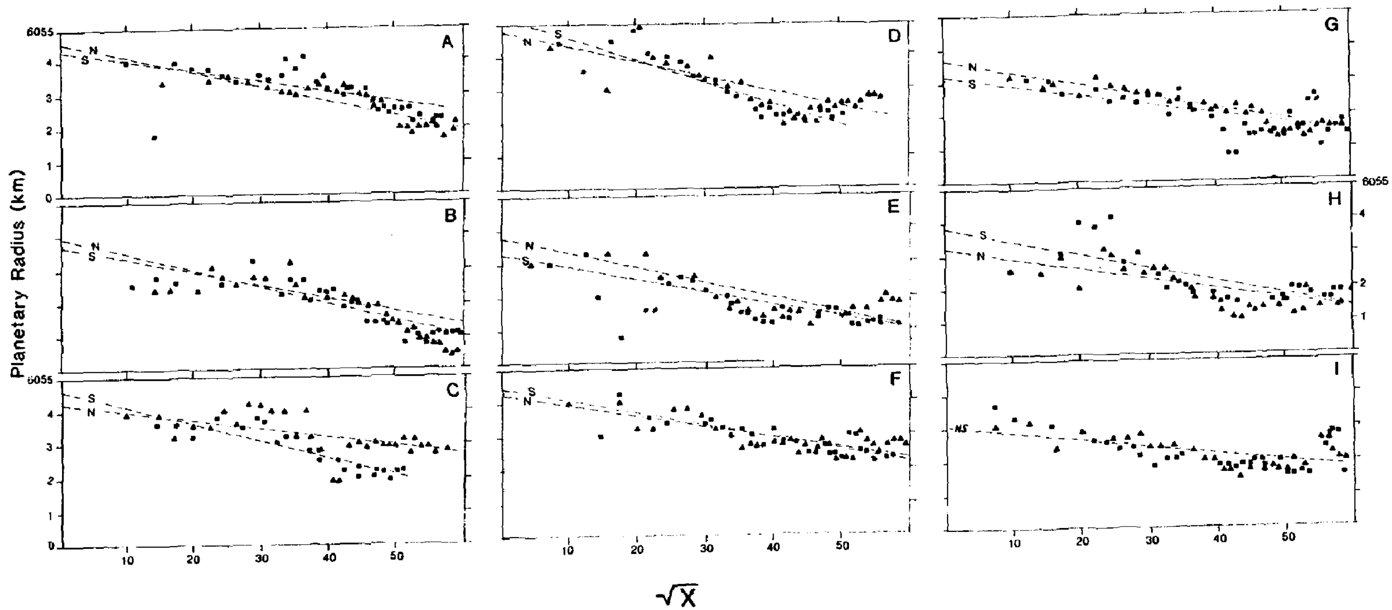

Fig. 7. Altimetry in profiles parallel to the linear discontinuities of Eastern Aphrodite plotted as a function of the square root of distance. Origin of the horizontal scale is the axes of symmetry shown in Figure 6D. Lines represent best-fitting least squares-determined linear trends through observed data. N = northern half; S = southern half. Correlation coefficients, slopes and ridge crest elevations, and estimated parameters are given in Table III.

The overall altimetric variations in Eastern Aphrodite in directions parallel to CSDs are small compared to areas of Western Aphrodite Terra (Grimm and Solomon, 1989), and the degree of fit between the elevation and the square root of distance out to 3600 km from the ridge crests approaches confidence levels of terrestrial bathymetry in similar correlations. In comparison with the typical form of terrestrial TBL topography, the slopes in profiles across Eastern Aphrodite Terra are shallower by a factor of 2 to 3, and the linear fit to the data in Eastern Aphrodite is correspondingly sensitive to altimetric variations.

5.2. Slope of Thermal Boundary Layer Topography

The surface slope (Δ) associated with the boundary layer of newly-created lithosphere decreases as the lithosphere cools, contracts, and subsides on either side of a divergent boundary such that

$$\Delta = 2pa\,\partial\mathrm{T}k/\pi)^{0.5}, \tag{1}$$

(Parsons and Sclater, 1977), where density is p, and thermal expansion coefficient and diffusivity are a and k, and ∂T is the temperature difference across the boundary layer. In addition to any variations in the thermal properties, lateral variations in density of the lithosphere or density of portions of it (crustal thickness) may result in a corresponding change in the estimate for Δ. Even assuming similar material thermal properties and spreading rate at divergent boundaries on Earth and Venus, the slope of the height/$\sqrt{x}$ relationship for TBL topography on Venus (Δ_V) will be reduced from its value on Earth (Δ_e) such that

$$\Delta_V/\Delta_e = 0.68 \text{ to } 0.82, \tag{2}$$

depending in part on the difference in mantle temperatures (T_m) but largely as a result of the higher average surface temperature ($T_s = 450°C$) on Venus. Values of Δ_e and Δ_V determined from altimetry and bathymetry are 300–350 m/m.y.$^{0.5}$ (Parsons and Sclater, 1977; Hayes, 1988) and 190–230 m/m.y.$^{0.5}$ (Table III) respectively, giving an observed value of $\Delta_V/\Delta_e = 0.5$ to 0.7 close to that predicted.

5.3. Rates of Spreading

The observed slopes and ridge crest altitude of Eastern Aphrodite (Figure 7 and Table III) are similar to those that would result from spreading rates (v) similar to the North Atlantic (1 to 2 cm/yr) and mantle temperatures warmer by 100° to 200° over comparable depths on Earth. Following Sotin *et al.* (1989) and Crumpler and Head (1990) the spreading rate associated with the observed slopes may be estimated from the relation between the observed slope and theoretical slope of the related TBL topography,

$$\Delta = [2a(T_m - T_s)\,(kx/\pi v)^{0.5}]. \tag{3}$$

The result of applying this equality to each of the observed profiles is listed in Table III for values of $a = 3.2 \times 10^{-5}$/K, $k = 10^{-6}\,\mathrm{m^2/s}$, $T_m = 1500°\,\mathrm{C}$, and $T_s =$

450° C. An observed characteristic of the estimated spreading rate in Table III is an inverse proportionality between the rate estimated from single profiles and the local correlation coefficient (r) between surface altitude, h, and the square root of the distance from the ridge crest, $\sqrt{x}$ suggesting that as the relief or topographic variance in the profiles becomes greater, the estimated slopes of the best-fitting linear trend through the altimetry appear flatter. Examining the observed correlation, $r^* = 0.7$, between v and r, we estimate that the spreading rate is 0.7 and 1.4 cm/yr for correlations between h and $\sqrt{x}$ greater than 0.9. These rates are similar to those in Western Aphrodite estimated on the basis of a similar analysis (Crumpler and Head, 1990) and the results of Sotin *et al.* (1989) from Western Aphrodite where a statistically well-defined rate of ~ 0.5 cm/yr was determined on the basis of averaging all the altimetric data within a single domain as a function of distance from the axis of symmetry. On the basis of the range of values assumed for the constants in Eq. (1) and the range of techniques that are applicable to evaluate the altimetry data, values of spreading rate within the range 0.5 to 1.5 cm/yr are indicated throughout Aphrodite Terra.

5.4. Consistent and Predictable Regional Topographic Relationships

Using these fundamental observations we may compare the predicted characteristics of Eastern Aphrodite Terra with the observed characteristics and with those known to occur in association with divergent boundaries. If the CSDs and offset of linear symmetry axes in Eastern Aphrodite are analogous to fracture zones and transform faults, then the altitude of the surface at a given distance from the ridge crest is predicted to be dependent on the sense and magnitude of the ridge crest offset. Regional steps in altimetry occur across transform faults and fracture zones on Earth because of the juxtaposition of lithospheres of differing age, thermal state, cooling rate, and TBL thickness. If the offsets in symmetry across CSDs are similar to offsets in TBL topography across transform faults and fracture zones, then we can predict the sense and magnitude of altimetric offsets that should occur in the surface in directions across CSDs on the basis of the predicted rate of topographic subsidence and surface slope.

We tested this model by calculating the predicted shape of the Arecibo altimetry profile and surface altitudes on the basis of the observed distance from the ridge axes to the Arecibo profile track. An average slope, $h/\sqrt{x}$ based on the results of Table III was assumed and the angle of the symmetry axes with respect to the profile track were assumed and taken into account. Comparison of altimetry predicted on this basis with observed altimetry for Arecibo profiles parallel to the ridge axis (Figure 8) shows that there are fundamental similarities in observed and in predicted altimetry and that the variations in regional profile characteristics are predictable using an offset thermal boundary layer model. The eastward observed monotonic fall in altimetry along the western half of the Arecibo profile P3 is predicted using this model from the consistent southward offset of the symmetry crest eastward of CSDs **8**, **13**, and **9** respectively. Further east the ridge crest shifts northward, between CSDs **14** and **10**, and the corresponding predicted increase in surface altitude is observed along the Arecibo profile in accordance with the increased proximity of the ridge crest to the altimetry track. The nominal symmetry axis shifts southward again eastward of CSD **10** before continuing northward into Atla Regio. As a consequence, the altimetry along the east-west profile track is predicted to briefly descend east of CSD **10**, and subsequently increase slowly as the distance between the profile and the ridge crest gradually decreases along an oblique intercept. These relations are observed.

That these observed abrupt steps in the altimetry are predicted from the presence of discontinuities in the map shape of the highlands several thousand kilometers away is a further indication that the CSDs influence the topographic characteristics of surrounding lowlands for several thousand kilometers along their strike. Comparison of altimetry thus predicted on this basis with observed altimetry for Arecibo profiles nearly parallel to the ridge axis (Figure 8) shows that there are fundamental similarities of the observed and predicted across-strike profiles, and that the variations in regional profile charactersitics are predictable using an offset thermal boundary layer model. This is additional evidence, in addition to the altimetric and SAR image discontinuities, that the CSDs continue as distinct features far from the highlands and further supports the interpretation that they represent fracture zones associated with transform faults offsetting linear zones of crustal spreading rather than transform accommodation zones associated with rifts.

Grimm and Solomon (1989) considered an additional test for the plate boundary characteristics of CSDs by noting that fracture zones and transform faults associated with motion of rigid plates on a sphere are constrained by Euler's theorem

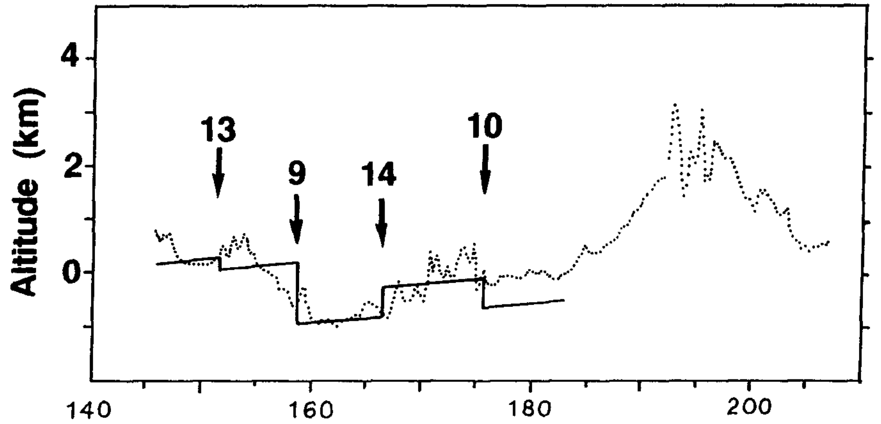

Fig. 8. Observed altimetry (dotted line) between CSDs along Arecibo high-resolution altimetry profile P3 (Figure 1B and Figure 5) compared with the predicted altimetry (solid lines) modeled as thermal boundary layer-type topography centered on the observed symmetry axes (Figure 6D) and offset along the mapped CSDs. The mapped location of the axes of symmetry show that the plateau-like rise of the lowland surface in the profile between CSDs **10** and **14** is a predicted consequence of the northward offset in the symmetry between CSDs **10** and **14**.

to follow small circles of arc described by rotation about a single pole. In general, the results show that no single pole of rotation may decribe the trace of all the observed CSDs in Western and Eastern Aphrodite Terra. In particular, given the accuracy of the location and orientation of individual CSDs, the CSDs in Eastern Aphrodite are generally congruent with a single pole of rotation if small deviations are permitted, but the same pole of rotation is inadequate for Western Aphrodite. On this basis, they suggest that a simple two plate model is not applicable for all of Aphrodite Terra or that one or more of the CSDs may act as deformable plate boundaries. Current resolutions are unable to address this question, and it must remain as a question to be resolved by the MAGELLAN data.

6. Comparison of Eastern and Western Aphrodite Terra

On the basis of large scale altimetric characteristics (Figure 1), there are some noteworthy similarities between Eastern and Western Aphrodite Terra. Both are characterized by (i) topographic segmentation of a central linear or elongate topographic rise, (ii) broad symmetry of a central high along a generally linear axial trend, (iii) a narrow and topographically complex axial high or ridge crest surrounded by broad flanking altimetrically low regions, (iv) a variety of extensional and volcanic features, (v) broad positive correlation of gravity and topography, (vi) distinct slopes and troughs where Arecibo profiles cross the projected trace of discontinuities and associated Pioneer Venus radar image linear discontinuities in the highland, and (vii) distinct changes in regional elevation across the trace of these discontinuities.

Differences in morphology, altimetry, and gravity between Eastern and Western Aphrodite Terra on the basis of Pioneer Venus altimetry, Pioneer Venus radar images, and Arecibo high-resolution altimetric profiles include: (i) Western Aphrodite Terra is dominated by plateaus compared to the ridge-like shape of Eastern Aphrodite Terra, (ii) the crest of Eastern Aphrodite Terra is in general 2 km lower in altitude, (iii) deep troughs or chasmata, such as Dali Chasma and Diana Chasma, interpreted to be extensional graben and rifts are more common and distinctive along the ridge-crest and flanks of Eastern Aphrodite, (iv) the lowland slopes on the north and south flank of Eastern Aphrodite Terra are topographically smoother and less complex than at equivalent distances in Western Aphrodite, and (v) apparent compensation depths suggest that Eastern Aphrodite is compensated at greater depths.

6.1. Characteristics of Western Aphrodite Terra

In Western Aphrodite Terra, the combination of CSD characteristics (Crumpler *et al.*, 1987), regional symmetry, symmetry offset and altimetric shapes, and variable wavelength of the symmetry (Crumpler and Head, 1988) were interpreted to be analogous to fractures zones, transform faults, thermal boundary layer topography, and segmentation of ridge crests characteristic of divergent plate boundaries resulting from relatively large horizontal separations of the crust along narrow zones of extensional deformation and crustal production (Head and Crumpler, 1987; Crumpler and Head, 1990). Evidence for divergent boundary characteristics in Western Aphrodite includes: (i) A series of parallel linear discontinuities similar to fracture zones each consisting of a trough- or scarp-like linear feature, associated regional topographic step up (or down) which cross the highlands extending for several thousand kilometers into the adjacent lowlands, and with the lateral offset similar to that predicted of newly-created lithosphere along transform faults at divergent ridge crests (Crumpler *et al.*, 1987); (ii) bilateral topographic symmetry across Aphrodite Terra over a variety of scales similar to that associated with thermal boundary layer topography frequently with superposed Iceland-like plateaus.

At least two scales of bilateral symmetry occur in association with divergent plate boundaries on Earth: (a) A broad regional symmetry in which the surface falls smoothly on either side of the plate boundary. This is the predicted general consequence of the cooling, contraction, and subsidence of newly-created lithosphere as it moves symmetrically and laterally away from the ridge crest; (b) small scale topographic elements bilaterally disposed about the ridge crest, often superimposed on the broad regional symmetry, and similar to paired oceanic plateaus that formed at a ridge crest (Kumar, 1979).

Profiles constructed parallel to the CSDs in Western Aphrodite Terra show several types of symmetry. Symmetry occurs in the relatively uniform downward slope of the surface away from the edges of the Equatorial Highlands and in the plateau-like form of the central highlands. Symmetrically arrayed linear axial troughs and bilateral ridges frequently occur on the plateau surface and are symmetric about the same axis as the more regional broad symmetry. A number of small altimetric and radar image features in the adjacent lowland slopes have mirror images 4000 to 6000 km away on the opposite flank of the equatorial lowland slopes.

6.2. Comparison of Eastern and Western Aphrodite Terra

On the basis of a comparison of the altimetric characteristics, the presence and distribution of CSDs, and the influence and comparisons of highland altimetry on the surrounding lowlands, Eastern and Western Aphrodite Terra reveal a number of similarities in morphology suggesting fundamental similarities in processes of their origin and evolution. Western Aphrodite is characterized by extensive plateaus with steep margins and variable scales of symmetry. Large scale symmetry occurs in Eastern Aphrodite and is a result of the observed correlation between altitude and the square root of distance on both the north and south flanks. In many cases the best fitting linear trend through altimetry data plotted as a function of the square root of distance is similar in slope and absolute altitude for both the north and south flanks.

We have tested this apparent similarity of Eastern and Western Aphrodite by

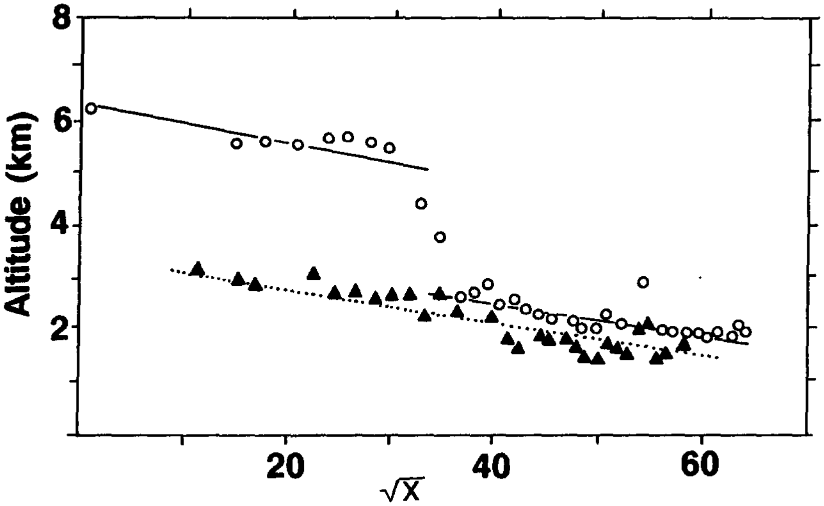

Fig. 9a.

taking the altimetry data from the north and south flanks of two profiles, one from Western Aphrodite and another from Eastern Aphrodite, averaging the north and south profile data in each case, and plotting the two profiles together on the same $h/\sqrt{X}$ plot. A comparison of both profiles (Figure 9a) reveals that in terms of absolute altitude, as well as overall slope, the lowland segments of the profiles are similar: The altitude of the surface at a distance of 1000 km to 4500 km from the axis of symmetry in both areas descends from about 6053 km to less than 6052 km, correlates linearly with the square root of distance from the corresponding axes of symmetry, and descend with similar slope. The surface between 0 and 1000 km in typical Western Aphrodite profiles lies 2 km above that of the surface lying at distances greater than 1000 km, but otherwise slopes at a rate similar to that of profiles in Eastern Aphrodite. The observed primary difference between the profiles in Western and Eastern Aphrodite Terra is the greater elevation of the central plateau of Western Aphrodite. As a consequence Western Aphrodite may be modeled as similar to Eastern Aphrodite but with a superposed plateau in the central ridge axis region (Figure 9b).

It is the bilaterally symmetric form of the central plateau-like highland that characterizes Western Aphrodite (Crumpler and Head, 1988; 1990). Symmetry associated with divergent boundaries is derived from two fundamental effects: (i) the bilateral process of crustal accretion and the corresponding bilateral similarity in thermal boundary layer evolution to either side of the ridge crest, and (ii) the splitting and separating of crustal thickness variations that arise from temporal and spatial variations in volcanic output along a ridge crest (Crumpler and Head, 1988). The observed similarities together with the differences between Eastern and Western Aphrodite Terra suggest that the primary difference between Eastern and Western Aphrodite may be in the volume rate of crustal production and the

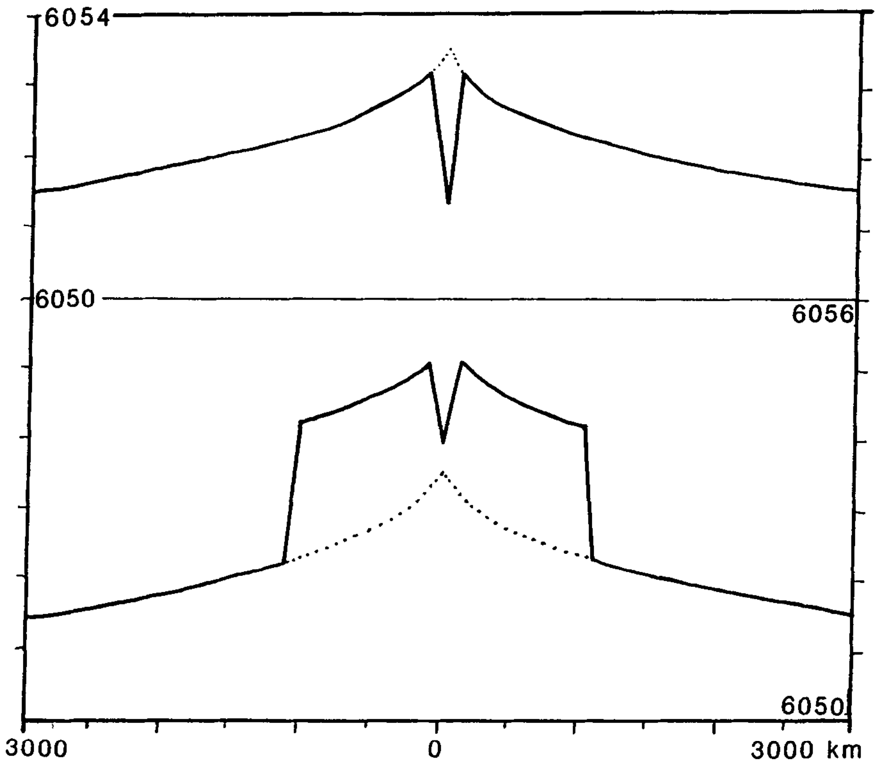

Fig. 9b.

Fig. 9. Interpretation of the similarities and differences between Eastern and Western Aphrodite. (A) Linear trend fitted to altimetric data derived from averages of the northern and southern halves of altimetry profiles from Western and Eastern Aphrodite. Data are plotted as a function of the square of distance (x) from the symmetry axis. Profiles in Western Aphrodite (open circles) consist of two components, a plateau and a sloping distal lower flank. Note that the altitude and slope of the profile from Western Aphrodite at distances greater than about 1000 km ($\sqrt{x} \approx 33$) is similar in altitude and in slope to profiles from Eastern Aphrodite (solid triangles). The altitude of the central region in Western Aphrodite is 2 km higher, but the slopes in both profiles at distances less than 1000 km are similar. (B) Inferred origin of similarities and differences between Eastern and Western Aphrodite. Variations of a few kilometers in altitude will reflect variations crustal thickness by a factor of two or three. Such variations in crustal thickness can occur as a result of a modest short-term increase in crustal production rates following a temporal increase in mantle temperature (plume or hot spot) beneath a spreading center.

corresponding isostatic elevation of the surface. Collectively these and other mirror-like or paired characteristics of altimetry and radar backscatter imply features initially formed at a divergent boundary and subsequently drifted apart over great distances. This supports the interpretation that the surface moves bilaterally away from a zone of crustal spreading and is mobile over great distances in contrast to simple rifts where lateral motion is limited.

The absolute difference in crustal thickness associated with differences in accretion history at divergent boundaries can be estimated as follows. If we assumed that Eastern Aphrodite represents simple divergence (absence of large anomalies in crustal production), then its average estimated ridge crest altitude, given from Table III, establishes the nominal height of a divergent ridge on Venus ($h_0 =$ 6053.9 km $\pm$ 0.9 km $\approx$ 6054 km). An altitude of the surface (h) which differs from this may be related to differences in the crustal thickness, Δc, from the Airy isostatic relation

$$h = h_0 + [(p_m - p_c)/p_m]\,\Delta c. \tag{4}$$

Assuming a density of 3300 and 3000 kg/m^{-3} for the mantle (p_m) and crust (p_c) and substituting the observed difference in nominal altitude (2 km) of plateaus in Western Aphrodite over the ridge crests of Eastern Aphrodite for h, the difference in crustal thickness (Δc) is estimated to be 20 km. These results, which are based on a generalized treatment of topography from profiles parallel to CSDs in Eastern Aphrodite, are similar to the estimated difference of 15 km in crustal thickness between 'normal' spreading centers and that resulting from enhanced crustal production at Western Aphrodite (Sotin *et al.*, 1989).

The variations in surface altitude associated with crustal thickness variations may be physical records of differences in the temperature of the mantle underlying the ridge crest in the past. On the basis of this model, the temperature of the mantle beneath the plateaus of Western Aphrodite (Ovda and Thetis Regio) is predicted to be approximately 100° C to 200° C warmer than that in Eastern Aphrodite throughout the formation of the elevated plateaus. Differences in mantle temperature would also influence the geophysical observables (viscosity, density, apparent depth of compensation, etc.) and, if present, should be apparent as distinct differences in the in the LOS gravity signature of Eastern and Westem Aphrodite.

Long-wavelength gravity on the seafloor is not in general strongly correlated with topography (exceptions include the North Atlantic; see for example, Rabinowitz and Jung, 1986) whereas gravity is highly correlated at long wavelengths with proposed regions of crustal spreading on Venus. A physical model reconciling these two observational differences is that there is deep plume-like mantle upwelling associated with large scale dynamic support and surlace crustal spreading along the length of Aphrodite Terra. This model predicts that most of the physical surface characteristic of divergent plate boundaries are present as on Earth, but differs in that divergent plate boundaries on Earth are largely passive plate-driven structures only infrequently correlating with plume-like convective upwelling. Where they do, as at Iceland, large positive gravity anomalies and greater apparent depths of compensation occur (Rabinowitz and Jung, 1986).

If convective upwelling is a component of the deep compensation mechanism on Venus through temperature-dependent viscous coupling (Kiefer and Hagar, 1988; Herrick *et al.*, 1989), then the observed apparent great depth of compensation in Eastern Aphrodite is, on this basis, a result of a correspondingly more viscous, and cooler (Kiefer and Hagar, 1989) mantle than that in Western Aphrodite Terra. This interpretation accords with the general results of Sotin *et al.* (1989) based on comparison of observed altimetry in Western Aphrodite with models of spreading center processes as they would appear in the Venus environment.

Chasmata are present in both Eastern and Western Aphrodite but are notably deeper and longer in Eastern Aphrodite. Sotin *et al.* (1989) noted that a central 200 km wide broad axial depression in Western Aphrodite is much wider than axial rifts which are characteristic of terrestrial spreading centers (tens of kilometers wide). They suggested that the greater width in Western Aphrodite may relate to either a recent decrease in the crustal production rates and a corresponding decrease in crustal thickness during the last 20 Myr, or because the crustal spreading process is distributed over a diffuse region rather than along a single graben. The extreme depth of chasmata in Eastern Aphrodite (1 to 2 km) might reflect a correspondingly more abrupt decrease in crustal thickness under the first model. Alternately, the similarity with chasmata of Beta Regio rift zones and relatively narrow widths of chasmata in Eastern Aphrodite could reflect a more focused and narrow zone of tectonic extension than that in Western Aphrodite possibly reflecting a rapid increase in crustal strain rates. In the latter case, if the magmatic supply lagged behind during rapid increases in spreading rate, correspondingly deep chasma would develop until eventually filled by associated volcanism. On the basis of great apparent depths of compensation, regional topographic slopes analogous to that associated with crustal spreading, and relatively smaller component of crustal thickness variations in Eastern Aphrodite relative to Western Aphrodite, we suggest that the current depth of chasmata in Eastern Aphrodite may reflect rapid increases in spreading rates. Rapid increase in local spreading rates and correspondingly greater tensile stress and rifting might be associated with dynamic ascent of underlying mantle plumes into a relatively cool and viscous overlying mantle. The associated crustal stress could be favorable to the eruption of magmas from subcrustal magma bodies in Eastern Aphrodite relative to that in Western Aphrodite. Either extrusive eruptions are relatively less common in Western Aphrodite (lower extrusive to intrusive ratio), or the width of the extension zone in Western Aphrodite could enhance more regional type eruptions at the expense of central vent type eruptions. The latter is supported by the fact that circular domical peaks interpreted to be volcanic edifices (Senske. 1989) are relatively more common in Eastern Aphrodite than in Western Aphrodite.

The arrival in the upper mantle of a warm upwelling would ultimately duplicate the conditions of warm upper mantle associated with mantle upwelling interpreted by Sotin *et al.* (1989) as responsible for the crustal thickness increases in the central region of Western Aphrodite. This interpretation predicts that the next stage in the evolution of Eastern Aphrodite might be an increase in volcanism, flooding of chasmata by extensive volcanic flows and constructs, associated crustal thickness increases, and plateau development resulting from an abrupt lateral increase in crustal thickness and isostatically supported greater surface altitude.

7. Discussion and Conclusions

Altimetric and radar image discontinuities, or CSDs, cut across the nearly east-west strike of Eastern Aphrodite Terra dividing or segmenting it into offset domains; and each domain is characterized by a discontinuous central chasma or trough. The central chasmata are frequently flanked by a pair of ridges. Pioneer Venus radar images of adjacent plains reveal that the discontinuities extend for several thousand kilometers off the highlands and in directions generally similar to the orientation of discontinuities previously described from Western Aphrodite Terra. Each domain is characterized by a different morphological assemblage of peaks, troughs, and ridges. Troughs or chasmata are up to 3 km deep, linear, located centrally on the ridge crest within each segment, and are interpreted to be rift valleys indicative of extension in directions parallel to the CSDs. Domical peaks up to 3 km high on the ridges flanking the chasma, are generally circular in plan, isolated, and similar to altimetric features mapped elsewhere in Arecibo and Venera images as large volcanic edifices. Eastern Aphrodite is altimetrically similar to other extensional tectonic environments identified on Venus such as Beta Regio. This is especially true of Atla Regio where a broad domical high is associated with several chasma and isolated peaks of probable volcanic origin.

Altimetric profiles across Eastern Aphrodite are more ridge-like than the plateaus of Western Aphrodite, but are characterized by both regional symmetry and symmetric ridges and troughs. Multiple parallel profiles show that the symmetry occurs along linear axes which are offset northward or southward at the CSDs in a manner analogous to the offset of divergent plate boundaries at transform faults and fracture zones. Distinct steps in the surface altitude occur across the CSDs both within the highlands and in the surrounding lowlands, and correspond to the offsets to the northwest and southeast that occur in the ridge crests along the strike of CSDs.

On the basis of the observed size and length of CSDs, the consistency of a variety of altimetry tests for thermal boundary layer topography, the magnitude of thermal boundary layer topography, the predicted way in which the altimetry is influenced by the highland offsets, and the evidence for symmetry at a variety of wavelengths, Eastern Aphrodite Terra is comparable to the predicted form of topography associated with crustal spreading processes in particular and a mobile and tectonically active crust in general. Additional evidence for the presence of divergent boundary characteristics and the fundamental characteristics of TBL topography throughout Eastern Aphrodite include the discontinuous nature of central chasma, their offsets at major highland discontinuities, the broad and detailed forms of symmetry, and the predictable relationships between the altimetry in directions across CSDs and the animetry in directions parallel to CSDs. The off-axis altimetric form of Eastern Aphrodite, the paired ridge-trough arrangement, and the domical peaks on chasma flanks are similar to known bathymetric features on divergent plate boundaries.

On the basis of this interpretation we tested whether the slope decreases are symmetrical in shape, with a functional form dependent on the square root of distance, and an absolute magnitude similar to that predicted for a divergent boundary-related thermal boundary layer topography under the surface conditions of Venus. The results reveal that the surface in Eastern Aphrodite decreases relatively symmetrically with distance from the crest in directions parallel to local CSDs (correlation coefficient ~ 0.75) and as a function of the square root of the distance from the central ridge crest. The altimetric profile shape and the slope of the surface in directions parallel to the discontinuities and perpendicular to the central chasmata are similar to that predicted from rates of divergence of 0.7 to 1.5 cm/yr. These rates are similar to those determined on the basis of analyses of gravity and topography in Western Aphrodite Terra (Crumpler and Head, 1989; Sotin *et al.*, 1989; Black *et al.*, 1989).

The dependence of the predicted sense and magnitude of the altimetry changes on observed CSD orientation in Figure 8 implies that the orientation of the CSDs exerts a significant influence on the local surface altitude in adjacent lowlands. In this respect, the CSDs together with their great length and parallel nature are similar to the known characteristics of fracture zones associated with transform faults and ridge crest offsets on the seafloor. This model was tested by comparing observed vertical surface offsets in Arecibo high-resolution altimetry profiles across several CSDs, with the vertical altimetry offsets predicted from simple models of surface altitude based on the assumption of crustal spreading from the regional ridge crest. A similar test was performed previously for Western Aphrodite (Crumpler and Head, 1990), and it was found that the regional altimetry generally behaved according to that predicted, but the additional contribution of off-axis topography associated with altimetric symmetry elements there resulted in local anomalous departures from the predicted altimetry. In Eastern Aphrodite, the agreement between predicted and observed altimetry is closer both across and parallel to the axis and reflects the absence of significant off-axis altimetric relief and small scale symmetry elements.

Based on the fit of topography in Eastern Aphrodite Terra to simple TBL models, the high correlation coefficient between topography and the square root of the distance from the ridge crest, and the similarity of observed profiles to predicted altitudes based on typical terrestrial spreading rates mapped to Venus conditions, Eastern Aphrodite is more comparable to divergence at 'normal' spreading centers where crustal production is relatively uniform. Western Aphrodite is more comparable overall to areas of anomalous crustal production at ridge crests (such as Iceland) where abundant volcanism results in a plateau-like anomalous crustal thickness and additional contributions to the topography over that resulting from TBL effects alone.

Variations in crustal production occur on Earth and crustal thicknesses greater than average are interpreted as being a response to anomalous mantle temperature structure beneath a spreading axis (Reid and Jackson, 1981; Sotin *et al.*, 1989).

The result is an increase in the relative volume rates of melt produced at a divergent boundary, increased local rates of volcanism and intrusion, and correspondingly increased lava and intrusive accumulation and crustal thickening (Reid and Jackson, 1981; Sotin *et al.*, 1989). The resultant increased local crustal volume production rates, and increased thickness of crust corresponds to an increase in the isostatically-supported surface altitude relative to that typical of the seafloor produced during nominal crustal spreading (Figure 9B). This type of ridge crest is relatively uncommon at present on Earth, but the abundance of oceanic plateaus, many of which represent anomalously thickened oceanic crustal sections in older seafloor (Nur and Ben Avraham, 1982; Moores, 1986; Sandwell and MacKenzie, 1989; Mahoney, 1987; Carlson *et al.*, 1980) suggest that plateau-forming anomalous ridge crest volcanism may frequently have occurred throughout the geologic history of the seafloor.

The divergent boundary characteristics of Eastern and Western Aphrodite Terra together extend for 14,000 km, which is more than a third of the combined great circle length of the Equatorial Highlands. A major question that we are currently assessing is whether the divergent boundary characteristics described from the Western and Eastern Aphrodite segments of the Equatorial Highlands are present in adjacent parts of the Equatorial Highlands to the east and west. The great east-west extent of divergent boundary characteristics and the evidence for large absolute horizontal motion of the surface away from the axis of spreading, implies that the Equatorial Highlands may have a potentially large-scale influence on the tectonic characteristics of a significant area of the surface of Venus. On the basis of similarities in radar backscatter characteristics, the surrounding lowlands and adjoining areas of tessera may be strongly influenced or related in origin to the processes operating within the Equatorial Highlands. Because of the inherent symmetry of the spreading process, this predicts that the tectonic and volcanic characteristics, age, elevation, and variations in crustal thicknesss in the southern hemisphere are likely to mirror the distribution of these characteristics imaged by Venera 15/16 and now known to occur in the 25% of the surface of Venus lying north of about 30° latitude. These interpretations and predictions may be further tested by Magellan observations.

We conclude that Eastern Aphrodite displays a variety of geological and geophysical characteristics similar to that occurring at divergent boundaries. These conclusions are independent of whether the lithosphere is strong and plate-like (plate-driven) or weak and plastic (convective-driven), and the current analysis does not specify in detail which style might be operating. The surface map characteristics are the result of great horizontal motion (spreading) of the crust diverging from a well-defined linear region, a process that can occur whether the surface is part of a thick and strong plate detached from mantle convection, as occurs on Earth in plate tectonics, or part of a thin and weak layer attached to a deep convective limb. The conclusion that the crust of Venus is horizontally mobile and that the crustal production occurs in linear zones implies that the surface of Venus differs substantially from the horizontally stable older lithospheres and surfaces associated with the smaller bodies in the inner solar system. This ultimately implies that Venus is more Earth-like in global tectonic style than the other terrestrial planets irrespective of its absolute rate or detailed differences compared to Earth.

Acknowledgments

The financial support of the National Aeronautics and Space Administration grants NGR-40-002-116 and NAGW-713, from the Planetary Geology and Geophysics Program of the Solar System Exploration Division, Office of Space Science and Applications, are gratefully acknowledged. Paul Fisher helped with PV data display and Peter Nievert helped with reproductions. Arecibo profiles were provided by John Harmon and Don Campbell. Jayne Aubele, Duane Bindschadler, David Senske, and Christophe Sotin discussed and suggested improvements on various earlier aspects of this work, and M. Ivanov and E. Stofan provided formal reviews resulting in many constructive suggestions for revisions to the final manuscript.

References

Arvidson, R. E., Plaut, J. J., Jurgens, R. F., Saunders, R. S., and Slade, M. A.: 1989, 'Geology of Southern Guinevere Planitia, Venus, Based on Analysis of Goldstone Radar Data', *Lunar Planet. Sci.* **XX**, 25.

Barsukov, V. L., Borunov, S. P., Volkov, V., Dorofeyva, V. A., Zolotov, M. Yu, Parotkin, S. V., Semenov, Yu. V., Sidorov, Yu. I., Khodakovsky, I. L., and Shapkin, A. I.: 1986, 'Estimation of Mineral Composition of Soil at Landing Sites of Venera 13, 14, and Vega 2 Landers According to Thermodynamical Calculations', *Doklady AN SSSR* **287**, 415.

Basilevsky, A.T., and Surkov, Y. A.: 1989, 'Chemical Compositions of Venusian Rocks and Some Geochemical Implications', *V-GRAM*, **15**, 2–4, Magellan Project-JPL

Basilevsky, A. T., Pronin, A. A., Ronca, L. B., Kryuchov, V. P., Sukhanov, A. L., and Markov, M. S.: 1986, 'Styles of Tectonic Deformation on Venus: Analysis of Venera 15 and 16 Data', *Jour. Geophys. Res.*, **91**, D399–411.

Bindschadler, D. L., and Head, J. W.: 1986, 'VEGA Landing Sites: Venera 15/16 Unit Analogs from Pioneer Venus Reflectivity and RMS Slope Data', *Geophys. Res. Lett.* **13**, 1415–1418.

Bindshadler, D. L., and Head, J. W.: 1988a, 'Diffuse Scattering of Radar on the Surface of Venus: Origin and Implications for the Distribution of Soils', *Earth, Moon, and Planets*, **42**, 133–149.

Bindschadler, D. L., and Head, J. W.: 1988b, 'Models for the Origin of Tesserae Terrain on Venus', *Lunar Planet Sci.* **XIX**, 78–79.

Bindschadler, D. L., and Head, J. W.: 1988c, 'Definition and Characterization of Subtypes of the Venus Tesserae', *Lunar Planet Sci.* **XIX**, 76–77.

Bindschadler, D. L., Head, J. W., Kreslavsky, M. A., Shkurotov, Yu. G., and Basilevsky, A. T.: 1990, 'Distribution of Tesserae Terrain on Venus: Prediction for Magellan', *Geophys. Res. Let.*, **17**, 171–174.

Black, M. T., Zuber, M. T., and McAdoo, D. C.: 1989, 'Comparison of Observed and Predicted Gravity Profiles over Aphrodite Terra', *Venus, Lunar Planet. Sci.* **XX**, 82–83.

Bowin, C.: 1983, 'Gravity, Topography, and Crustal Evolution of Venus', *Icarus*, **56**, 345–371.

Bosworth, W.: 1989, 'Basin and Range Style Tectonics in East Africa', *Jour. African Earth Sci.* **8**, 191–201.

Campbell, D. B., Head, J. W., Hine, A. A., Harmon, J. K., Senske, D. A., and Fisher, P. C.: 1989, 'Styles of Volcanism on Venus: New Arecibo High Resolution Radar Data', *Science*, **246**, 373–377.

Campbell, D. B., Head, J. W., Harmon, J. K. and Hine, A. A.: 1984, 'Venus: Volcanism and Rift Formation in Beta Regio', *Science*, **226**, 167–170.
Carlson, R. N., Christiansen, N., and Moore, R.: 1980, 'Anomalous Crustal Structures in Ocean Basins: Continental Fragments and Oceanic Plateaus', *Earth Planet. Sci. Lett.* **51**, 171–180.
Crumpler, L. S., Head, J. W. and Harmon, J. K.: 1987, 'Regional Linear Cross-Strike Discontinuities in Western Aphrodite Terra', *Geophys. Res. Lett.*, **14**, 607–610.
Crumpler, L. S., and Head, J. W.: 1988, 'Bilateral Symmetry Patterns Across Aphrodite Terra, Venus', *J. Geophys. Res.*, **93**, 301–312
Crumpler, L. S., and Head, J. W.: 1990, 'Spreading Center and Divergent Plate Boundary Characteristics in Western Aphrodite Terra, Venus: Further Analysis of Topography, Morphology, Symmetry, and Map Patterns', submitted to Tectonophysics, in press.
Ehmann, W. J.: 1983, 'Aphrodite Terra, Venus: Characteristics and Geologic Provinces', M.S. thesis, Brown University.
Garvin, J. B., and Bryan, W. B.: 1987, 'Venus Surface Compositions: Implications from Terrestrial Geochemical Analogies', *Astron. Vestnik.*, **11**, 122–135.
Grimm, R. E., and Solomon, S. C.: 1989, 'Tests of Crustal Divergence Models for Aphrodite Terra, Venus', *J. Geophys. Res.*, **94**, 12, 103–12, 131.
Hagfors, T.: 1970, 'Remote Probing of the Moon by Microwave and Infrared Emissions and Radar', *Radio Sci.* **5**, 189–227.
Hayes, D. E.: 1988, 'Age-Depth Relationships and Depth Anomalies in the Southeast Indian Ocean and South Atlantic Ocean', *Jour. Geophys. Res.* **93**, 2937–2954.
Head, J. W.: 1990, 'Venus Trough and Ridge Tessera: Analog to Earth Ocean Crust Formed at Spreading Centers?', *Jour. Geophys. Res.*, **95**, 7119–7132.
Head, J. W., and Crumpler, L. S.: 1989, 'Divergent Plate Boundary Characteristics and Crustal Spreading in Aphrodite Terra, Venus: a Test of Some Predictions, *Earth, Moon, and Planets*, **44**, 219–231.
Head, J. W., and Crumpler, L. S.: 1987, 'Evidence for Divergent Plate Boundary Characteristics and Crustal Spreading on Venus', *Science*, **238**, 1380–1385.
Head, J. W., Garvin, J. B., Campbell, D. B., Pettengill, G. H., Masursky, H., Saunders, R. S., Barsukov, V. L., Basilvesky, A. T. and Surkov, Y. A.: 1987, 'Vega Landing Sites: Geological Characteristics of the Surrounding Region, Rusalka Planitia, Venus', *Lunar Planet. Sci.* **XVII**, 327–328.
Head, J. W.: 1986, 'Venus Global Tectonics: Tectonic Style and Evidence for Latitudinal Distribution of Tectonic Features', *Lunar Planet. Sci.* **XVII**, 325–326.
Head, J. W., Peterfreund, A. R. and Garvin, J. W.: 1985, 'Surface Characteristics of Venus Derived from Pioneer Venus Altimetry, Roughness, and Reflectivity Measurements', *Jour. Geophys. Res.*, **90**, 6873–6885.
Herrick, R. R., Bills, B. G., and Hall, S. A.: 1989, 'Variations in Effective Compensation Depth across Aphrodite Terra, Venus', *Geophys. Res. Lett.*, **16**, 543–546.
Hess, P. C., and Head, J. W.: 1989, 'Derivation of Primary Magmas and Melting of Crustal Materials on Venus: Some Preliminary Considerations', *28th International Geol. Congress Abstracts*, **2**, 55.
Kaula, W. K., and Phillips, R. J.: 1981, 'Quantitative Tests for Plate Tectonics on Venus', *Geophys. Res. Lett.*, **8**, 1187–1190.
Kiefer, W. S., and Hager: B. A., 1989, 'Mantle Plumes on Venus: A Model for the Equatorial Highlands and a Possible Connection with Ovoids', *Lun. Planet. Sci.* **IX**, 601–602.
Kiefer, W. S., Richards, M. A., Hager, B. H. and Bills, B. G.: 1986, 'A Dynamic Model of Venus' Gravity Field', *Geophys. Res. Lett.*, **13**, 14–17.
Kondrat'yev, K. Y., Krupenio, N. N. and Selivanov, A. S.: 1987, *The Planet Venus*, (in Russian), Gidrometeoizdat Publishing, Leningrad, U.S.S.R., 277 pp.
Kumar, N.: 1979, 'Origin of "Paired" Aseismic Rises: Ceara' and Sierra Leone Rises in the Equatorial, and the Rio Grande Rise and Walvis Ridge in the South Atlantic', *Mar. Geol.*, **30**, 175–191.
Lewis, B. T. R.: 1979, 'Periodicities in Volcanism and Longitudinal Magma Flow on the East Pacific Rise at 23N', *Geophys. Res. Lett.*, **6**, 753–756.
Macdonald, K. C.: 1982, 'Mid-Ocean Ridges: Fine Scale Tectonic, Volcanic and Hydrothermal Processes within the Plate Boundary Zone', *Ann. Rev. Earth Planet. Sci.* **10**, 155–190.

Mahoney, J. J.: 1987, 'An Isotopic Survey of Pacific Oceanic Plateaus: Implications for their Nature and Origin', in H. Keating, P. Fryer, R. Batiza, and G. W. Boehlert, (eds.), *Seamounts, Islands, and Atolls*, *Geophys. Monogr.* **43**, Am. Geophys. Union, Washington, pp. 207–220.

Malinverno, A.: 1990, 'A Quantitative Study of the Axial Topography of the Mid-Atlantic Ridge', *Jour. Geophys. Res.* **95**, 2645–2660.

Masursky, H., Eliason, E., Ford, P. G., McGill, G. E., Pettengill, G. H., Schaber, G. G. and Schubert G., 1980, 'Pioneer Venus Radar Results: Geology from Images and Altimetry', *J. Geophys. Res.*, **85**, 8232–8260.

McGill, G. E., Steenstrup, S. J., Barton, C. and Ford, P. G.: 1981, 'Continental Rifting and the Origin of Beta Regio, Venus', *Geophys. Res. Lett.* **8**, 737–740.

McGill, G. E., Warner, J. L., Malin, M. C. Arvidson, R. E., Eliason, E., Nozette, S., and Reasenberg, R. D.: 1983, 'Topography, Surface Properties, and Tectonic Evolution', in D. M. Hunten, L. Colin, T. M. Donahue, and V. I. Moroz, (eds.), *Venus*, Univ. Arizona Press, Tucson: Chap. 6.

Moores, E. M.: 1986, 'The Proterozoic Ophiolite Problem, Continental Emergence, and the Venus Connection', *Science*, **234**, 65–68.

Nur, A., and Ben-Avraham, Z.: 1982, 'Oceanic Plateaus, the Fragmentation of Continents, and Mountain Building', *Jour. Geophys. Res.*, **87**, 3644–3667.

Parsons, B. and Sclater, J. G.: 1977, 'An Analysis of the Variation of Ocean Floor Bathymetry and Heat Flow with Age', *Jour. Geophys. Res.*, **82**, 803–827.

Pettengill, G. H., Eliason, E.., Ford, P. G., Loriot, G. B., Masursky, H., and McGill, G. E.: 1980, 'Pioneer Venus Radar Results: Altimetry and Surface Properties, *Jour. Geophys. Res.*, **85**, 8261–8270.

Pettengill, G. H., and Ford, P. G.: 1985, 'Pioneer Venus Altimetry Data', NSSDC 78-051A-02D.

Phillips, R. J., and Malin, M. C.: 1983, 'The Interior of Venus and Tectonic Implications', Chap. 10, In D. M. Hunten, L. Colin, T. M. Donahue, and V. I. Moroz, (eds.), *Venus*, Univ. Arizona Press, Tucson: 159–214.

Phillips, R. J., Kaula, W. M., McGill, G. E., and Malin, M. C.: 1981, 'Tectonics and Evolution of Venus', *Science*, **212**, 879–887.

Pockalny, R. A., Detrick, R. S. and Fox, P. J.: 1986, 'Punctuated Magmatism and the Generation of Ridge Axis Topography along the Mid-Atlantic Ridge', *Eos Trans. AGU* **67**, 1213.

Rabinowitz, P. D., and Jung, W. Y.: 1986, 'Gravity Anomalies in the Western North Atlantic Ocean', in P. R. Vogt, and B. E. Tucholke, eds., *The Geology of North America, volume M, The Western North Atlantic*, Geol. Soc. America, Chapter 13.

Reasenberg, R. D., Goldberg, Z. M., MacNeil, P. E., and Shapiro, I. I.: 1981, 'Venus Gravity: A High Resolution Map', *Jour. Geophys. Res.*, **86**, 7173–7179.

Reid, I., and Jackson, H. R.: 1981, 'Oceanic Spreading Rate and Crustal Thickness', *Mar. Geophys. Res.*, **5**, 165–172.

Sandwell, D. T., and MacKenzie, K. R., 'Geoid Height Versus Topography for Oceanic Plateaus and Swells', *Jour. Geophys. Res.*, **94**, 7403–7418.

Saunders, R. S., Sjogren, W. L. and Trager, G. B.: 1988, 'Venus Equatorial Highlands: Systematic Longitudinal Trend in Compensation Mechanism', *EOS* **69**, 1295.

Schaber, G. G.: 1982, 'Venus: Limited Extension and Volcanism along Zones of Lithopsheric Weakness', *Geophys. Res. Lett.*, **9**, 499–502.

Senske, D. A.: 1989, 'Geology of the Equatorial Region of Venus: A Comparison of Volcanic and Tectonic Styles between the Equatorial Region and Northern High Latitudes, M.S. Thesis, Brown University.

Senske, D. A. and Head, J. W.: 1989, 'Venus Equatorial Geologic Units', *Lunar Planet. Sci.*, **XX**, 986–987.

Sjogren, W. L., Bills, B. G., Birkeland, P. W., Nottinger, N. A., Ritke, S. J., and Phillips, R. J.: 1983, 'Venus Gravity Anomalies and their Correlation with Topography, *Jour. Geophys. Res.*, **88**, 1119–1128

Sotin, C., Senske, D. A., Head, J. W., and Parmentier, E. M.: 1989, 'Terrestrial Spreading Centers under Venus Conditions: Evaluation of a Crustal Spreading Model for Western Aphrodite Terra', *Earth Planet. Sci. Lett.*, **95**, 321–333.

Stofan, E. R., Head, J. W., Campbell, D. B., Zisk, S. H., Bogomolov, A. F., Rzhiga, O. N.,

Basilevsky, A. T., and Armand, N.: 1989, 'Geology of a Rift Zone on Venus: Beta Regio and Devana Chasma', *Geol. Soc. Am. Bulletin*, **101**, 143–156.
Surkov, Y. A., Moskalyova, L. P., Shcheglov, O. P., Dudin, A. D., Kharyukova, V. P., Manelyan, O. S., and Smirnov, G. G.: 1986, 'Study of Composition of Venusian Rock in Northern Part of Aphrodite Terra by Vega 2 Lander', *Pis'ma v AZH*, **12**, 66.
Vogt, P. R.: 1979, 'Global Magmatic Episodes: New Evidence and Implications for Steady-State Mid-Ocean Ridge', *Geology*, **7**, 93–98.